LUND UNIVERSITY

DEPARTMENT OF ASTRONOMY AND THEORETICAL PHYSICS

BACHELOR THESIS

Properties of two Higgs Doublet Models in relation to data on $B \to D\tau\nu$

Author:
Joel Oredsson

Supervisor:
Johan Rathsman

January 30, 2014

Abstract

In this thesis we investigate the properties of a specific two Higgs Doublet Model (2HDM) that can be used to explain the data on $B \to D\tau\nu$ and $B \to D^*\tau\nu$, which deviate from the Standard Model (SM) by 3.4σ. The 2HDM is the simplest extension of the Standard model scalar sector. Phenomenologically it is very rich with 4 new Higgs bosons: 2 neutral and an electromagnetic charged pair. The 2HDMs exhibits tree-level flavor changing neutral currents (FCNC) which are constrained by experiments and therefore need to be suppressed in the model. These FCNC depends on the masses of the Higgs bosons and the couplings in the Yukawa sector. We investigate the possible mass spectrum of the model by requiring vacuum stability, tree-level unitarity and perturbativity, as well as making sure the model is within limits of the experimental electroweak precision tests. Then we use renormalization group equations (RGEs) to evolve the Yukawa couplings to see when they reach the limits set by FCNC.

Contents

Abbreviations

2HDM
Two Higgs Doublet model

BSM
Beyond Standard Model

CP
Charge-Parity

FCNC
Flavor Changing Neutral Currents

LHC
Large Hadron Collider

RGE
Renormalization Group Equation

SM
Standard Model

VEV
Vacuum Expectation Value

QCD
Quantum ChromoDynamics

QED
Quantum ElectroDynamics

QFT
Quantum Field Theory

1 Populärvetenskaplig introduktion

Vår värld beskrivs idag på den mest fundamentala nivån av kvantfältteori. Den förenar två av fysikens fantastiska upptäckter, kvantmekaniken och den speciella relativitetsteorin. Efter hårt arbete av fysiker under 1900-talet kom det fram att allting runt omkring oss kan beskrivas som fält, vars excitationer motsvarar partiklar. Alla partiklar har sitt eget fält och vibrationer i ett fält kan orsaka vibrationer i ett annat. Partikelfysiker försöker beskriva dessa interaktioner så fullkomligt som bara går.

Experimentellt har man funnit att det finns fyra sorters fundamental växelverkan i naturen. Elektromagnetism och gravitation är krafter som vi upplever i vår vardag medan den svaga samt starka växelverkan är lite mindre kända. Den svaga orsakar flera fenomen så som vissa atomsönderfall och den starka är kraften som håller ihop alla atomkärnor.

Under åren som gått har en modell växt fram som beskriver elektromagnetism och den svaga samt starka växelverkan: Standardmodellen. Den har passerat många experimentella krävande tester genom åren med oerhörd precision i vissa områden. Men trots sin succé så är det klart att den inte är fullkomlig. För det första så saknas en kvantbeskrivning av gravitationen. Det finns även andra bevis för så kallad fysik bortom Standardmodellen t.ex. mörk materia/energi och varifrån neutrinos får sin massa.

2012 upptäcktes en av Standardmodellens viktigaste byggstenar: Higgsbosonen. Denna partikel är en excitation av dess underliggande Higgsfält vilket spelar en stor roll i Standardmodellen. Genom interaktioner med detta fält får nämligen alla partiklar(utom neutrinos) sin massa genom något som kallas Higgsmekanismen. Denna mekanism är något av en grund för Standardmodellen som förenar elektromagnetism och den svaga växelverkan till ett gemensamt fenomen.

Men upptäckten av en Higgsboson skulle kunna vara bara början vad gäller Higgspartiklar. Det finns nämligen argument för att utöka Standardmodellens Higgsmekanism till att innehålla flera Higgsfält. Ett av dessa argument kommer från Supersymmetri som är en populär teori för att lösa vissa av Standardmodellens problem. Supersymmetri kräver nämligen minst två Higgsfält.

När man introducerar ett extra Higgsfält i Standardmodellen får man många nya fenomen så som fyra nya Higgspartiklar varav två är elektriskt laddade. Dessa partiklar är intressanta fenomenologiskt genom att de kan ge bidrag till processer som i sådana fall inte borde stämma överens med Standardmodellen. Därmed skulle nya Higgspartiklar vara ett klart tecken på fysik bortom Standardmodellen.

Inom partikelfysiken används ofta statistiska verktyg när man ska analysera stora mängder data. Partiklar kan sönderfalla på många olika sätt och i studier av B mesonen[1] så skiljer sig de experimentella resultaten mot beräkningar med Standardmodellen. Man fann att den sönderföll till en D meson, en tau och en neutrino fler gånger än väntat[2].

En förklaring till detta som föreslagits är en modell med två Higgsfält vilket skulle innebära att en B meson kan sönderfalla genom en laddad Higgspartikel och således förklara experimenten. Denna kandidatuppsats undersöker en sådan Dubbelhiggsmodell för att se hur den beter sig vid högre energier och i förhållande till andra experiment.

Parameterområdet är stort för Dubbelhiggsmodeller men det finns många begränsningar som man kan göra. Vi undersöker bland annat huruvida modellens grundtillstånd är stabilt och om modellen är inom ramarna för experimentella värden på fenomen så som mesonmixningar[3]. Att ta hänsyn till detta resulterar i gränser för de nya Higgsbosonernas massor.

I kvantfältteorin så är parametrarna beroende av vid vilken energi experimenten utförs. Detta gör så att modeller kan utvecklas och bete sig vitt skilt åt vid olika energier. Till exempel så blir den elektromagnetiska kraften starkare vid högre energier medan den starka växelverkan blir svagare. Så man måste definiera sin modell vid en specifik energi vilket kallas Renormering och med så kallade renormeringsgruppekvationer(RGE) kan man sedan se hur parametrarna beror på energin.

Vi undersöker Dubbelhiggsmodellens RGE-utveckling för att undersöka hur modellen klarar av de gränser vi funnit. En attraktiv modell skulle åtminstone klara sig fint vid alla energier som är aktuella experimentellt. Om modellen skulle vara ostabil vid högre energier skulle det kunna tyda på att den inte är den kompletta bilden eller att parametrarna är finjusterade så att modellen endast är meningsfull vid låga energier.

[1] En B meson är en partikel som består utav två kvarkar vilket kan jämföras med protoner och neutroner som består utav tre kvarkar.

[2] D är också en meson medan tau är en tyngre kusin till elektronen och neutrinon är en väldigt lätt elektriskt neutral partikel.

[3] Ett kvantmekaniskt fenomen som innebär att de elektriskt oladdade mesonerna är i en superposition av två olika tillstånd. De kan därmed oscillera till deras motsvarande antipartikel.

2 Introduction

In 2012 the first fundamental scalar particle was discovered at the Large Hardon Collider (LHC) [1] [2]. So far it is all in agreement with predictions according to the Standard Model (SM). In the SM there is a single Higgs Doublet field that gives rise to mass terms for all of the fermions[4]. To increase this sector of the SM can seem unnecessary, but the Standard model has some problems which can be solved by a theory called Supersymmetry, and introducing Supersymmetry requires at least one extra Higgs field to account for all the fermion masses. Supersymmetry has been around for a long time and many people hoped that it will be discovered at the LHC. A rigorous experimental investigation of the Higgs sector can thus give the first clues of supersymmetrical theories.

However the general two Higgs Doublet Model (2HDM) exhibits tree-level flavor changing neutral currents (FCNC) which are constrained by experiments. One way to avoid these FCNC is to impose a Z_2 symmetry on the model which can be done in four different ways. In this thesis we investigate the specific 2HDM type III which is 2HDM type II with a broken Z_2 symmetry. It has been shown recently [3] that this specific model could be used to explain the latest data on the decays $B \to D\tau\nu$ and $B \to D^*\tau\nu$. This is an interesting case since this data is in disagreement with the SM by 3.4σ and could therefore be evidence of new physics beyond the SM [4].

The FCNC currents of the 2HDMs are depending on the mass spectrum of the Higgs particles and the couplings in the Yukawa sector. To see what masses are possible for the Higgs bosons we consider other experimental constraints from requiring vacuum stability, unitarity and perturbativity. We also take into account constraints from electroweak precision tests. This results in different mass spectrum scenarios. The FCNC are mostly constrained by neutral meson mixing and we calculate the precise limits on the Yukawa couplings in three mass scenarios.

We use renormalization group equations (RGEs) to investigate how stable the 2HDM type III is under evolution of the Yukawa couplings in the mentioned three scenarios. A large sensitivity in the parameter space could be a sign of fine tuning or instability of the model.

The structure of this thesis is as follows.

First of in section 3 we give a quick review of the SM Higgs model. This is not treated in detail and is mostly a reminder of how the process of spontaneous symmetry breaking gives rise to the masses of gauge bosons and fermions. This can easily be skipped by anyone familiar with the subject.

Next in section 4 we review the general theory of 2HDM. We also discuss the relevant B meson decays that is in a disagreement with the SM and how 2HDM type III can explain this.

In section 5 we investigate in more detail what kind of constraints can be set on the parameters in 2HDM. We discuss the vacuum stability, unitarity and perturbativity of the model as well as how it affect the electroweak precision parameters S and T. The limits on the masses of the H and A boson are presented.

[4]Except neutrinos. Even though they have small masses, they are treated like massless particles in the SM.

Section 6 explains how we evolve the Yukawa couplings with RGE to see how the model behaves at higher energies and the results are presented in sextion 7

The details about the computations done in the thesis can be found in the appendices. A goes through the steps of how the 2HDM type III contributes to the taunic B decays. We also explain what software we used to do the RGE evolution and list all the input that was used in B and C.

3 Spontaneous Symmetry Breaking

There are several good books about QFT and particle physics that explains spontaneous symmetry breaking and the Higgs mechanism. A few favorites ranging in difficulty are [5], [6] and [7]. One should not forget though that the subject of symmetry breaking is a widely used concept that exists in many areas of physics.

Symmetry is very important and spontaneous symmetry breaking occurs in many places in nature[5]. Whenever the laws of a physical system are invariant under a transformation that transformation corresponds to a symmetry. However that symmetry may be lost if the system undergoes a spontaneous process where it ends up in an asymmetrical state. For example the Lagrangian can have a certain symmetry but, depending on the potential, the fields ground state may not exhibit the same symmetry. Hence the term spontaneously broken symmetry.

To see this phenomenon in quantum field theory we can consider the *linear sigma model*. Though being very simple it shows the mechanism of spontaneous symmetry breaking. It is basically a field that acquires a Vacuum Expectaion Value (VEV) by being in the ground state of the potential. So one can expand the model around the VEV instead of the origin.

The model consists of N real scalar fields $\phi^i(x)$ with the Lagrangian(implicit sum over the is)

$$\mathcal{L} = \frac{1}{2}\partial_\mu\phi_i\partial^\mu\phi^i + \frac{1}{2}\mu^2\phi_i\phi^i - \frac{\lambda}{4}\left(\phi_i\phi^i\right)^2. \tag{1}$$

Where we take λ and μ to be real.

The ϕ^i fields are gathered in a vector and since this Lagrangian only contains scalar products of that vector one can see that the model exhibits a $O(N)$ symmetry(rotations of the ϕ vector). However this symmetry will be broken because the potential

$$V(\phi^i) = -\frac{1}{2}\mu^2\phi_i\phi^i + \frac{\lambda}{4}\left(\phi_i\phi^i\right)^2 \tag{2}$$

is minimized when

$$\phi_i\phi^i = \frac{\mu^2}{\lambda} = v^2. \tag{3}$$

[5]A widely spread explanation is the example of a ferromagnet. If the temperature is high enough the magnetic moments in the material is disorganized and the system is therefore rotationally invariant. But if the magnet is cooled down below the Curie temperature the spins becomes spontaneously aligned. The system is then magnetic and is no longer rotationally invariant.

This sets the length of the vector ϕ. So the possible VEV of the model is the surface of an N dimensional sphere. In the case of two fields this can easily be visualized by the so called Mexican hat or Wine bottle potential, see fig. 1.

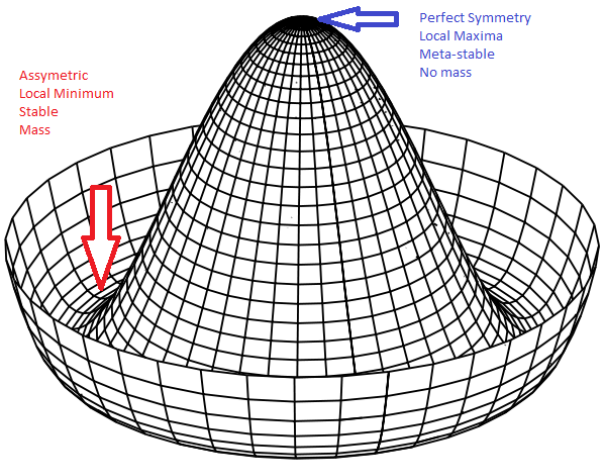

Figure 1: A visualization of the Higgs potential in two dimensions. One can clearly see how the ground state is not as symmetrical as the top of the hat. At the top one can move the field along any direction and expect the same behavior but in the bottom of the slope one can move the field along a circle and still be in the minima. It turns out that exciting the field in the radial direction will correspond to Higgs bosons. Picture taken from [8].

Since the surface of a N dimensional sphere is N-1 dimensional the vacuum configuration of the field, i.e. a point on the N dim sphere, is not invariant under $O(N)$ transformations anymore. To see the consequences of breaking the symmetry we pick an arbitrary point on the N dim sphere and expand the field around that point. This can be done by setting the minimal configuration to be a constant value in the Nth direction, $\phi_0 = (0, \ldots, 0, v)$. This breaks the $O(N)$ symmetry down to $O(N-1)$(rotation of all zero value components). So now we can expand around this minima like $\phi = (\pi(x), v + \sigma(x))$, where π is a $N-1$ dimensional vector. With these new fields we can rewrite the Lagrangian[6].

$$\mathcal{L} = \frac{1}{2}\left(\partial_\mu \pi^k\right)^2 + \frac{1}{2}\left(\partial_\mu \sigma\right)^2 - \frac{1}{2}(2\mu)^2\sigma^2 - \sqrt{\lambda}\mu\sigma^3 - \frac{\lambda}{4}\sigma^4 + \sqrt{\lambda}\mu\left(\pi^k\right)^2\sigma - \frac{\lambda}{2}\left(\pi^k\right)^2\sigma^2 - \frac{\lambda}{4}\left[\left(\pi^k\right)^2\right] \quad (4)$$

Notice the non existing mass terms for the π^k. The VEV broke the continuous $O(N)$ symmetry and $N-1$ massless scalar fields appeared. This can all be stated exactly with *Goldstone's theorem*. It says that for every spontaneously broken continuous symmetry, the theory must contain a massless particle which is called a Goldstone boson. In the case of the linear sigma model, $O(N)$ has a continuous symmetry for a rotation in every plane and there are $N(N-1)/2$ of them. So the

[6]We throw away any constant terms since they have no effect on the equations of motion.

VEV breaks $N-1$ of them(the difference of independent continuous symmetries in $O(N)$ and $O(N-1)$).

3.1 The Higgs Mechanism

The SM is built up by three symmetries, $SU(3)_C \times SU(2)_L \times U(1)_Y$. These are so called gauge symmetries or local symmetries. They are local in the sense that the Lagrangian of the SM is invariant under any transformation of the gauge group which can be different for every point in spacetime. When one impose these local symmetries on the theory one is also forced to introduce new fields to make the Lagrangian invariant. These fields are called gauge fields and their particles are what we associate with forces in nature.

This works great for the strong and electromagnetic forces. One can build a $SU(3) \times U(1)$ invariant model which would introduce two gauge fields whose particles would correspond to the gluon and photon. However the weak force exists and the particles associated with it are massive. The process of creating massive gauge bosons is governed by the Higgs mechanism. It uses both spontaneous symmetry breaking and local symmetries to create the massive W and Z bosons. The massless photon is also incorporated in the process as well as all the fermion masses.

The Higgs mechanism is built around the Higgs field(a scalar field), which acquires a VEV because of its potential. The Higgs mechanism in the SM uses one Higgs field that transforms as a $SU(2)_L$ doublet and is in a sense the most minimal Higgs sector possible. The most general renormalizable potential that gives a VEV to the field is

$$V(\Phi) = -\mu^2 \Phi^\dagger \Phi + \lambda \left(\Phi^\dagger \Phi\right)^2 . \tag{5}$$

Where the minimum of the potential occurs at $\Phi^\dagger \Phi = \frac{1}{2}\sqrt{\frac{\mu^2}{\lambda}}$.

The Φ field has also got an $U(1)$ symmetry so its complete gauge transformation can be written as

$$\Phi \to e^{i\alpha^a \tau^a} e^{i\beta} \Phi. \tag{6}$$

Where $\tau^a = \frac{\sigma^a}{2}$ are the generators of $SU(2)$. The α^a and β are just some arbitrary real parameters that are dependent on spacetime and hence the term local symmetry.

This transformation is composed of 4 continuous symmetries, one for each generator of the group. The field is conventionally expanded around the minimum as

$$\Phi = \frac{1}{2} \begin{pmatrix} 0 \\ v + h(x) \end{pmatrix} \tag{7}$$

The trained eye can see that the actual minimum where $h(x) = 0$ is invariant under the specific choice of gauge transformation $\alpha_1 = \alpha_2 = 0$, $\alpha_3 = 2\beta$. This is a set of invariant transformations that are still present after the electroweak symmetry breaking. Hence one continuous symmetry remains but the other 3 symmetries are

broken and one therefore get 3 Goldstone bosons. However this time they do not correspond to any physical particles. Because one can always rotate the Φ field to only have a real component as in eq. 7. Instead the Goldstone bosons gets "eaten" by the gauge bosons which become massive[7].

So the SM Higgs mechanism breaks the initial $SU(2)_L \times U(1)_Y$ to one remaining symmetry $U(1)_\gamma$ which gives one massless gauge boson (photon) and the three massive particles corresponds to the weak force carriers $W^\pm$ and Z. The remaining degree of freedom in the Higgs field is the Higgs boson, $h(x)$.

However the fact that the charged weak current only couples to left handed particles can be achieved by letting the left handed and right handed fermions be in different representations of the $SU(2)_L$ gauge group. The left handed fermions are in $SU(2)$ doublets while the right handed ones are $SU(2)$ singlets.This is at first sight pretty troublesome since it makes terms like

$$m\bar{e}_L e_R$$

in the Lagrangian forbidden since it is not gauge invariant. However this is solved elegantly by making the fermions acquire mass from the VEV of the Higgs field with terms like

$$g\bar{L}_L \cdot \Phi e_R.$$

Where $L_L = \begin{pmatrix} \nu_e \\ e_L \end{pmatrix}$ is a doublet with the left handed leptons in it and g is a Yukawa coupling. The details works the same way as in the 2HDM which is treated more in detail in the next section.

This minimal Higgs model was implemented in the late 60s by Glashow, Weinberg and Salam[8]. It unites electromagnetism and the weak force into one beautiful electroweak theory. But, as will be discussed in the next section, it may not be the complete picture of the scalar sector.

[7]A massless spin 1 particle has two degrees of freedom corresponding to its two possible helicities. But a massive spin 1 particle has three degrees of freedom. So the gauge bosons gets an extra degree of freedom when it eats the Goldstone bosons. That the Goldstone bosons completely disappear is a consequence of how the Lagrangian is gauge fixed. They are still there in other gauge choices to cancel out effects of other unphysical particles.

[8]Even in the absence of the discovery of any Higgs boson they were jointly awarded the Nobel prize in 1979 because of the description of the electroweak interactions that was in agreement with experiments and also the prediction of the neutral current.

4 2HDM

The reason to extend the scalar sector of the SM may not be clear immediately. The SM Higgs mechanism is simple in the way that given all the fermion masses the only free parameter is the Higgs mass. But when a second scalar field is introduced the number of parameters is increased substantially. The main motivation for doing this comes from Supersymmetry. In supersymmetric theories a single Higgs doublet can not account for the masses of both the charge -1/3 and +2/3 quarks. So you need at least one more Higgs doublet. The model we are investigating in this thesis contains two Higgs doublets and is used in the so called minimal supersymmetric standard model (MSSM).

The Higgs sector is very interesting now when the LHC is up and running. The discovery of a Higgs particle at 126 GeV may only be the beginning. After the LHC has been upgraded new energy scales can be probed and new particles can be found. Phenomenologically 2HDM is very rich compared to the SM Higgs with charged Higgs bosons, pseudo scalars, different decay modes and branching ratios. The parameter space of 2HDM is also bigger and it will take some time to search through all the possible scenarios, if it is at all possible.

Since it is a hot area of research there is a much written about 2HDMs in recent years. A good review that covers the most popular 2HDMs is [9]. As the name suggest the scalar sector of 2HDMs consists of two $SU(2)$ doublet scalar fields $\Phi_{1,2}$ with hypercharge +1. The most general renormalizable potential can be written

$$\begin{aligned} V &= m_{11}^2\Phi_1^\dagger\Phi_1 + m_{22}^2\Phi_2^\dagger\Phi_2 - (m_{12}^2\Phi_1^\dagger\Phi_2 + h.c.) \\ &+ \frac{1}{2}\lambda_1\left(\Phi_1^\dagger\Phi_1\right)^2 + \frac{1}{2}\lambda_2\left(\Phi_2^\dagger\Phi_2\right)^2 + \frac{1}{2}\lambda_3\left(\Phi_1^\dagger\Phi_1\right)\left(\Phi_2^\dagger\Phi_2\right) + \frac{1}{2}\lambda_4\left(\Phi_1^\dagger\Phi_2\right)\left(\Phi_2^\dagger\Phi_1\right) \\ &+ \left\{\frac{1}{2}\lambda_5\left(\Phi_1^\dagger\Phi_2\right)^2 + \lambda_6\left(\Phi_1^\dagger\Phi_1\right)\left(\Phi_1^\dagger\Phi_2\right) + \lambda_7\left(\Phi_2^\dagger\Phi_2\right)\left(\Phi_1^\dagger\Phi_2\right) + h.c.\right\}. \end{aligned} \quad (8)$$

Here the parameters m_{11}, m_{22} and $\lambda_{1,2,3,4}$ are real while m_{12} and $\lambda_{5,6,7}$ are complex in general. So this potential has 14 degrees of freedom from the 6 real and 4 complex parameters. However note that this number can be decreased by assuming certain symmetries and requiring absence of CP violation. For example we can impose a Z_2 symmetry on the Φ fields, making one odd and one even. That would get rid of m_{12}^2 and $\lambda_{6,7}$. However one usually keep m_{12}^2 non-zero because compared to $\lambda_{6,7}$ it only breaks the Z_2 symmetry softly. If we require no CP violation it is sufficient, although not necessary, for the parameters to be real which would result in 8 degrees of freedom. One can note though that certain degrees of freedom disappear since the VEV and one Higgs boson mass are fixed by experiments.

The $\Phi_{1,2}$ are $SU(2)$ doublets and the minimization of eq. 8, i.e. the vacuum expectation values of the fields, are

$$\langle\Phi_1\rangle = \frac{1}{\sqrt{2}}e^{i\theta_1}\begin{pmatrix}0\\v_1\end{pmatrix}, \qquad \langle\Phi_2\rangle = \frac{1}{\sqrt{2}}e^{i\theta_2}\begin{pmatrix}0\\v_2\end{pmatrix}. \quad (9)$$

Where we from here on out set $\theta_1 = \theta_2 = 0$ to avoid spontaneous CP violation.

The $\Phi_{1,2}$ fields in the general setup are indistinguishable so it is always possible to define a orthonormal linear combination of the fields without modifying the

physics. One useful basis is the Higgs basis where only one of the fields get a VEV. This is done in section 4.1 when we investigate the Yukawa sector.

A useful and important definition is an angle β from

$$\tan\beta \equiv \frac{v_2}{v_1} \tag{10}$$

which measures the rotation from the general basis to the Higgs basis. In the general 2HDM this is however not a physical parameter since the $\Phi_{1,2}$ fields are indistinguishable. But if there are any symmetries that distinguishes the two fields $\tan\beta$ becomes a physical parameter.

The Φ fields consists of 8 real fields. After electroweak symmetry breaking 3 of these corresponds to the Goldstone bosons that gets "eaten" by the familiar gauge bosons $W^{\pm}$ and Z^0. But now there are also 5 new scalar fields which can be divided into two CP even scalars h and H, one CP odd pseudo-scalar A and a pair of charged scalars $H^{\pm}$. To diagonalize the CP eigenstates we introduce an angle α so that the expansion of the fields can be written

$$\begin{aligned}\Phi_1 &= \begin{pmatrix} -s_\beta H^+ \\ \frac{1}{\sqrt{2}}(c_\beta v - s_\alpha h + c_\alpha H - i s_\beta A) \end{pmatrix}, \\ \Phi_2 &= \begin{pmatrix} c_\beta H^+ \\ \frac{1}{\sqrt{2}}(s_\beta v - c_\alpha h + s_\alpha H + i c_\beta A). \end{pmatrix}\end{aligned} \tag{11}$$

Where we have used the short notation $\sin\alpha \equiv s_\alpha$ and $\cos\alpha \equiv c_\alpha$ and similarly for β.

As already mentioned these are defined to have weak hyper charge $+1$. To couple these to both up and down quarks we need doublets with weak hyper charge -1 which can be created out of the complex conjugate fields.

$$\tilde{\Phi}_i = i\sigma_2 \Phi_i^* \tag{12}$$

The angles α and β are very important in phenomenology. For a detailed study of the subject one can look in [10]. Some of the most important points can quickly be pointed out though. Many vertices that couple the Higgs bosons to gauge bosons are proportional to $\cos(\beta-\alpha)$ and $\sin(\beta-\alpha)$. A list of the angle dependent vertices can be seen in table 1. Assuming that the 126 GeV Higgs is the lightest scalar particle requires roughly $\sin(\beta-\alpha) > 0.9$, which suppresses a lot of processes for example HWW and HZZ couplings. This can make it very hard to discover the neutral H boson. The decoupling limit $\sin(\beta-\alpha) = 1$ makes the h couplings to SM particles the same as in the SM.

4.1 The Yukawa Sector

The Yukawa sector is the part of the Lagrangian which describes how the scalar fields are being coupled to the fermion fields. Just as in the SM the left handed and right handed fermions are in different representation of the gauge group and therefore can not couple together to create gauge invariant mass terms. But with a $SU(2)$

$\cos(\beta-\alpha)$	$\sin(\beta-\alpha)$
W^+W^-H	W^+W^-h
ZZH	ZZh
ZAh	ZAH
$W^\pm H^\mp h$	$W^\pm H^\mp H$
$ZW^\pm H^\mp h$	$ZW^\pm H^\mp H$
$\gamma W^\pm H^\mp h$	$\gamma W^\pm H^\mp H$

Table 1: A list of vertices that couple Higgs particles and gauge bosons. The left ones are proportional to $\cos(\beta-\alpha)$ while the right ones are proportional to $\sin(\beta-\alpha)$.

doublet scalar field one can create gauge invariant terms which after electroweak symmetry breaking creates mass terms for the fermions in the same way as in the SM.

The fermions in SM can be written as:

$$\begin{aligned} Q_L &= \begin{pmatrix} U_L \\ D_L \end{pmatrix} & U_R, D_R \\ L_L &= \begin{pmatrix} \nu_L \\ E_L \end{pmatrix} & E_R \end{aligned} \tag{13}$$

The most general Yukawa interactions is one where both Higgs fields couple to every fermion field. To make the equations visually appealing we leave the generation index implicit on the fermions and Yukawa couplings $\eta^F_{1,2}$. All fermions are vectors in 3 dimensional generation space and the Yukawa couplings are 3×3 matrices in the same space. So the Yukawa sector Lagrangian can be written as[9]

$$\begin{aligned} \mathcal{L}_Y = &-\bar{Q}_L\cdot\tilde{\Phi}_1\eta_1^U U_R - \bar{Q}_L\cdot\Phi_1\eta_1^D D_R - \bar{L}_L\cdot\Phi_1\eta_1^L E_R \\ &-\bar{Q}_L\cdot\tilde{\Phi}_2\eta_2^U U_R - \bar{Q}_L\cdot\Phi_2\eta_2^D D_R - \bar{L}_L\cdot\Phi_2\eta_2^L E_R + h.c. \end{aligned} \tag{14}$$

It can be convenient to write the general Yukawa sector in the Higgs basis where only one Higgs field has a VEV. This makes it easy to see the diagonal terms in the Lagrangian since there is only one VEV that can create mass terms. The Higgs basis are related to the general basis by a rotation of the Higgs fields

$$\begin{aligned} H_1 &= \cos\beta\Phi_1 + \sin\beta\Phi_2 \\ H_2 &= -\sin\beta\Phi_1 + \cos\beta\Phi_2. \end{aligned} \tag{15}$$

Now only H_1 has a VEV, $\langle H_1\rangle = \frac{1}{\sqrt{2}}\begin{pmatrix} 0 \\ v \end{pmatrix}$ where $v^2 = v_1^2 + v_2^2$. Then the Yukawa interaction becomes

$$\begin{aligned} \mathcal{L}_Y = &-\bar{Q}_L\cdot\tilde{H}_1\kappa_0^U U_R - \bar{Q}_L\cdot H_1\kappa_0^D D_R - \bar{L}_L\cdot H_1\kappa_0^L E_R \\ &-\bar{Q}_L\cdot\tilde{H}_2\rho_0^U U_R - \bar{Q}_L\cdot H_2\rho_0^D D_R - \bar{L}_L\cdot H_2\rho_0^L E_R + h.c. \end{aligned} \tag{16}$$

[9]We treat neutrinos as massless so they do not couple to the Higgs field.

The mass terms should arise from the H_1 terms and we can therefore go over to a fermion mass basis where the κ^F Yukawa coupling matrices are diagonal. This can always be done with some unitary matrices V_L^F, V_R^F acting on the fermion vectors. But in general we can not diagonalize both the κ^F and the ρ^F matrices simultaneously. This can be a big problem since it can give rise to FCNC at tree level. The new matrices are

$$\kappa^F = V_L^F \kappa_0^F V_R^{F\dagger} = \frac{\sqrt{2}}{v} M_{ii}^F, \tag{17}$$

$$\rho^F = V_L^F \rho_0^F V_R^{F\dagger}. \tag{18}$$

Where the matrix M^F has the physical fermion masses along its diagonal. We also define the CKM matrix

$$V_{CKM} \equiv V_L^U V_L^{D\dagger}. \tag{19}$$

If we expand the Higgs fields in the physical fields we can write down the Lagrangians Yukawa sector where we can read of the interactions directly.

$$\begin{aligned}
\mathcal{L}_Y = &- \frac{1}{\sqrt{2}}\bar{U}\left[\kappa^U s_{\beta-\alpha} + (\rho^U P_R + \rho^{U\dagger} P_L) c_{\beta-\alpha}\right] Uh \\
&- \frac{1}{\sqrt{2}}\bar{U}\left[\kappa^U c_{\beta-\alpha} - (\rho^U P_R + \rho^{U\dagger} P_L) s_{\beta-\alpha}\right] UH + \frac{i}{\sqrt{2}}\bar{U}\left(\rho^U P_R - \rho^{U\dagger} P_L\right) UA \\
&- \frac{1}{\sqrt{2}}\bar{D}\left[\kappa^D s_{\beta-\alpha} + (\rho^D P_R + \rho^{D\dagger} P_L) c_{\beta-\alpha}\right] Dh \\
&- \frac{1}{\sqrt{2}}\bar{D}\left[\kappa^D c_{\beta-\alpha} - (\rho^D P_R + \rho^{D\dagger} P_L) s_{\beta-\alpha}\right] DH - \frac{i}{\sqrt{2}}\bar{D}\left(\rho^D P_R - \rho^{D\dagger} P_L\right) DA \\
&- \frac{1}{\sqrt{2}}\bar{L}\left[\kappa^L s_{\beta-\alpha} + (\rho^L P_R + \rho^{L\dagger} P_L) c_{\beta-\alpha}\right] Lh \\
&- \frac{1}{\sqrt{2}}\bar{L}\left[\kappa^L c_{\beta-\alpha} - (\rho^L P_R + \rho^{L\dagger} P_L) s_{\beta-\alpha}\right] LH - \frac{i}{\sqrt{2}}\bar{L}\left(\rho^L P_R - \rho^{L\dagger} P_L\right) LA \\
&- \left\{\bar{U}\left[V_{CKM}\rho^D P_R - \rho^{U\dagger} V_{CKM} P_L\right] DH^+ + \bar{\nu}\rho^L P_R L H^+ + h.c.\right\}
\end{aligned} \tag{20}$$

Where P_R and P_L are the projection operators, $(1 \pm \gamma_5)/2$. Here the U,D and L are Dirac spinors which carry a generation index as before.

In eq. 20 it is clear that non-diagonal ρ^F can induce tree-level FCNC. This is a problem phenomenologically because it would contribute to various processes such as decays of particles that are otherwise in agreement with the SM. Later on we will compute the limits on these non-diagonal elements by considering $F^0 - \bar{F}^0$[10] mixing and it turns out that there are strict constraints on some of these elements. The tree-level FCNC therefore need to be avoided or suppressed somehow.

One fix to these FCNC is to impose a Z_2 symmetry on the theory [11]. That would get rid of several terms in the general Yukawa Lagrangian, eq. 14, so that the up/down quarks couple to different Higgs fields. After diagonalization to the mass

[10] $F^0 - \bar{F}^0$ meaning neutral meson mixing, where F is K, D, B_d or B_s.

Type	U_R	D_R	L_R	ρ^U	ρ^D	ρ^L
I	+	+	+	$\kappa^U \cot\beta$	$\kappa^D \cot\beta$	$\kappa^L \cot\beta$
II	+	−	−	$\kappa^U \cot\beta$	$-\kappa^D \tan\beta$	$-\kappa^L \tan\beta$
Y	+	−	+	$\kappa^U \cot\beta$	$-\kappa^D \tan\beta$	$\kappa^L \cot\beta$
X	+	+	−	$\kappa^U \cot\beta$	$\kappa^D \cot\beta$	$-\kappa^L \tan\beta$

Table 2: A table of Z_2 symmetries that can be imposed on the 2HDM. Φ_1 is odd or -1 and Φ_2 is even or $+1$. For every type of Z_2 symmetry the ρ^F matrices become proportional to the κ^F matrices hence diagonal.

eigenstates the ρ^F matrices becomes proportional to the diagonal κ^F matrices thus making them diagonal as well.

There exists four possibilities of Z_2 symmetries that can be imposed on a 2HDM. These are listed in table 2. In this thesis we investigate the consequences of breaking the Z_2 symmetry of 2HDM type II which is the one used in MSSM. Just as stated previously this introduces FCNC at tree-level which from experiments are shown to be very small.

Cheng and Sher introduce an ansatz to naturally suppress the FCNC of 2HDM [12]. Since the diagonal couplings in κ^F have a hierarchy to them it is natural to assume this for the ρ^F as well. This can be done by relating the coupling to the masses of the associated fermions like

$$\rho^F_{ij} = \lambda^F_{ij} \sqrt{\frac{2m_i m_j}{v^2}}. \tag{21}$$

Where the λ^F_{ij} should be of order one. It is now known as the Cheng-Sher ansatz and naturally suppresses the non-diagonal couplings. The limits from meson mixings on some of the non-diagonal λ^F_{ij} are computed in section 5.2.

4.2 B meson decays explained with 2HDM

Searches at so called B meson factories where rare decays involving flavor observables are probes of new physics. The 2HDMs can have serious effects on some of these decays since they give rise to new particles. Recently the BABAR collaboration has done studies on the data on semileptonic B decays $B \to D\tau\nu$ and $B \to D^*\tau\nu$ [4]. For the ratios

$$\mathcal{R}(D) = \frac{\mathcal{B}(B \to D\tau\nu)}{\mathcal{B}(B \to Dl\nu)}, \tag{22}$$

they found the results in table 3. Both of the ratios disagree with the SM and combining them gives a 3.4σ deviation from the SM predictions [4].

These decays are both tree level processes in the SM. This makes it difficult to invent new physics to explain the experimental results. Because if the new physics should have size-able contributions one in general need a tree level process, i.e. a new charged particle. But introducing a new particle can have severe effects phenomenologically.

	$\mathcal{R}(D)$	$\mathcal{R}(D^*)$
Experiment(BABAR [4])	$0.440 \pm 0.058 \pm 0.042$	$0.332 \pm 0.024 \pm 0.018$
Theory(SM [4, 13, 14])	0.297 ± 0.017	0.252 ± 0.003

Table 3: Comparison between theory and experiment for the decays $B \to D\tau\nu$ and $B \to D^*\tau\nu$. For the experiment the first error is statistical and the second one is systematic. Combining both ratios gives a 3.4σ deviation between SM and experiment [4].

This is where the 2HDMs come into play. They introduce new charged scalar particles, $H^{\pm}$, that contribute to the decay of B mesons, see fig. 2 for an example of a tree-level process. But their couplings to fermions are proportional to the fermions mass which explains why they would only contribute to the taunic decays.

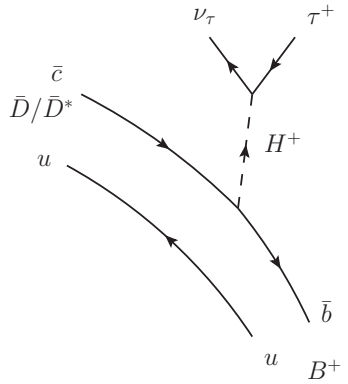

Figure 2: Example of B decay involving a charged scalar particle. In the SM there is a similar process where the b quark decays through a W^+.

The well studied 2HDM Type II has been favored a long time among the 2HDMs. It avoids unwanted FCNC but is unsatisfactory when it comes to the B decays. It cannot explain both $\mathcal{R}(D)$ and $\mathcal{R}(D^*)$ simultaneously [4] for any value of $\tan\beta$ and m_{H^+}, see fig. 3 [15].

But another 2HDM could be used to explain these decays. A breaking of the Z_2 symmetry would result in a 2HDM type III. Although such a model exhibits tree-level FCNC they can still be candidates if those currents are suppressed i.e. if the symmetry breaking is soft enough. The non-diagonal elements would contribute constructively to the B decays in question as we will show in the next section.

4.3 2HDM Type III

If the 2HDM is created without any discrete symmetries it is simply the most general 2HDM which ones Lagrangian we have already written down. However since the models without tree-level FCNC have been favored for such a long time and been given the names type I and type II, the most general model is now known as 2HDM

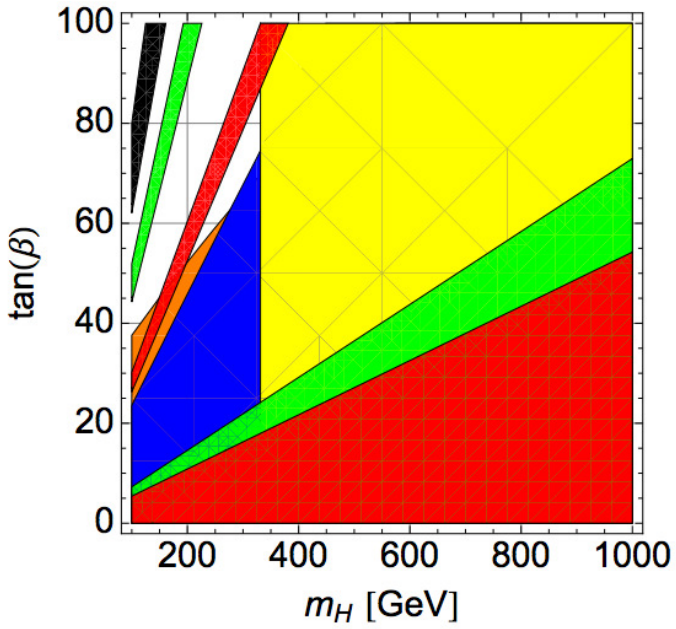

Figure 3: Constraints on 2HDM type II in the $\tan\beta$-m_H parameter space. Allowed regions from experiments are: $b \to \gamma s$ (yellow), $B \to D\tau\nu$ (green), $B \to \tau\nu$ (red), $B_s \to \mu^+\mu^-$ (orange), $K \to \mu\nu/\pi \to \mu\nu$ (blue) and $B \to D^*\tau\nu$ (black). Note that no region of the parameter space is compatible with all the decays. Plot taken from [15].

type III.[11]

As mentioned before the problem of this model is that it has dangerous FCNC but that can be fixed by making the neutral scalar masses heavy or assuming that the Yukawa couplings obey the Cheng-Sher ansatz. This requirement to suppress the FCNC to within experimental limits forces the non-diagonal elements of the Yukawa couplings to be small hence making the model resemble 2HDM type II a lot.

To explain both $\mathcal{R}(D)$ and $\mathcal{R}(D^*)$ a 2HDM of type III has been considered [3] where the authors parametrized a breaking of the Z_2 symmetry of 2HDM type II with the couplings ϵ^F. The quark Yukawa sector can then be written

$$\begin{aligned}\mathcal{L}_Y = &- \bar{Q}_L Y^U \tilde{\Phi}_U U_R - \bar{Q}_L Y^D \Phi_D D_R \\ &- \bar{Q}_L \epsilon^U \tilde{\Phi}_D U_R - \bar{Q}_L \epsilon^D \Phi_U D_R + h.c.\end{aligned} \tag{23}$$

where the 2HDM type II is recovered in the limit $\epsilon^{U,D} \to 0$ where there are separate Higgs field that couples to the up/down quarks.

The Lagrangian in eq. 23 can be expanded in the mass eigenstates of $\Phi_{U,D}$ as

[11]The 2HDM type Y and X are sometimes also named type III and IV. But to avoid confusion that is avoided in this thesis.

before which results in the Feynman rule in fig. 4 with

$$\Gamma^{H^\pm LR}_{u_f d_i} = \sum_{j=1}^{3} s_\beta V_{fj} \left[\frac{m_{d_i}}{c_\beta v} \delta_{ji} - (\tan\beta + \cot\beta)\epsilon^D_{ji} \right], \tag{24}$$

$$\Gamma^{H^\pm LR}_{d_f u_i} = \sum_{j=1}^{3} c_\beta V^*_{jf} \left[\frac{m_{u_i}}{s_\beta v} \delta_{ji} - (\tan\beta + \cot\beta)\epsilon^U_{ji} \right] \tag{25}$$

and $\Gamma^{H^\pm LR}_{q_f q_i} = \Gamma^{H^\pm RL\,*}_{q_i q_f}$.

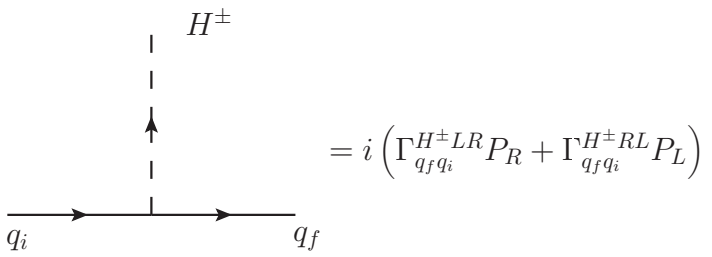

Figure 4: Feynman rule for the coupling of quarks to $H^\pm$.

In a possible B decay through a H^+, like in fig. 2, one integrates out the heavy scalar particle in an effective field theory since the B decays occur on a energy scale way below the electroweak scale. The procedure is a subject in itself and will not be treated in detail here. But the interested reader can find a sketch of the calculation of 2HDM contributions to the relevant B decays in Appendix A.

There is however some important points that should be pointed out about fitting the 2HDM type III to $\mathcal{R}(D)$ and $\mathcal{R}(D^*)$. The contributions are calculated with the vertices given by eq. 24-25 which of course depends on the ϵ^U and ϵ^D. But in the effective vertices the mass of the virtual H^+ particle is included as well. In the end the fit in [3] uses fixed values of $m_{H^\pm} = 500$ GeV and $\tan\beta = 50$. While all the other parameters of the model can be adjusted. The allowed regions in the parameter space of ϵ^U_{32} obtained in [3] can be seen in fig. 5.

The Yukawa couplings in eqs. (24 - 25) can be related to the basis used in eq. 20 which shows the breaking of the Z_2 symmetry more explicitly.

$$\Gamma^{H^\pm LR}_{u_f d_i} = \tan\beta V_{CKM} \left[\kappa^D - (\tan\beta + \cot\beta)\epsilon^D\right] = -V_{CKM}\rho^D, \tag{26}$$

$$\Gamma^{H^\pm RL}_{u_f d_i} = \cot\beta \left[\kappa^U - (\tan\beta + \cot\beta)\epsilon^U\right] V_{CKM} = \rho^{U\dagger} V_{CKM}, \tag{27}$$

or

$$\rho^D = -\tan\beta \left[\kappa^D - (\tan\beta + \cot\beta)\epsilon^D\right], \tag{28}$$

$$\rho^U = \cot\beta \left[\kappa^U - (\tan\beta + \cot\beta)\epsilon^{U\dagger}\right]. \tag{29}$$

Here it is very clear that in the limit $\epsilon^{U,D} \to 0$ the ρ matrices become proportional to the κ matrices just like in table 2.

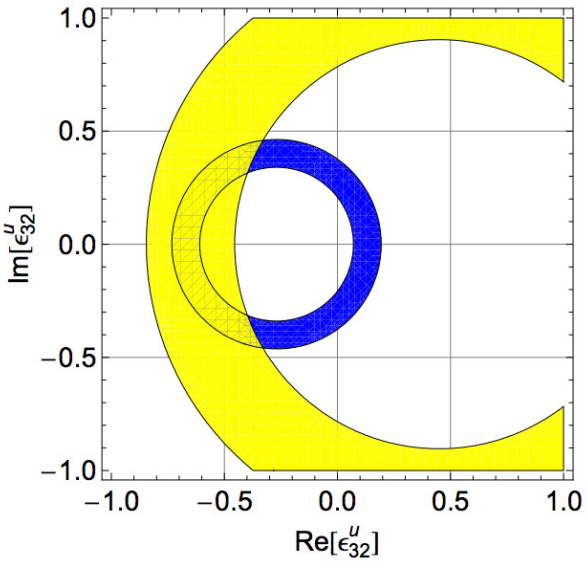

Figure 5: The allowed regions for the parameter ϵ^U_{32} fitting it to the data on $\mathcal{R}(D)$ (blue) and $\mathcal{R}(D^*)$ (yellow) using eqs. (47 - 48), $m_{H^\pm} = 500$ GeV and $\tan\beta = 50$. Plot taken from [3].

5 Constraints on 2HDM

Before evolving the ϵ^F with the RGEs we need to consider experimental constraints. To compute the limits on the non-diagonal elements of ϵ^F we need to know what masses we might expect for the Higgs bosons. To find that out, we consider other phenomenons that can put constraints on how light or heavy the H and A particles can be.

5.1 Stability, Unitarity, Perturbativity and Oblique Parameters

The 2HDM introduce a lot of new parameters to the scalar sector compared to the SM. By analyzing the limits on the λ_i one can find the possible mass-spectrum of the Higgs particles. Different constraints can be found in a recent review of 2HDMs [9] and constraints specifically for 2HDM type III in [15]. We list here a short summary of some of these constraints.

Stability of the vacuum

A general requirement for any field theory is that the potential should be bounded from below. Meaning that it does not go to $-\infty$ in any direction in the field space, thus making sure that the VEV of the field is stable. For the SM Higgs model this is easily satisfied because of the positive ϕ^4 term in the potential[12]. It gets a little bit more complex in the 2HDM model since there are a lot more parameters in

[12]The ϕ^4 term can actually turn negative at high energies through RGE evolution. However the vacuum is at least meta-stable [16].

the potential. But it turns out that sufficient conditions for stability can be found. Given that the hard Z_2 breaking terms $\lambda_{6,7} = 0$, the potential is bounded from below if the following conditions are satisfied [17]:

$$\begin{aligned} \lambda_1 &> 0, \\ \lambda_2 &> 0, \\ \lambda_3 &> -\sqrt{\lambda_1 \lambda_2}, \\ \lambda_3 + \lambda_4 - |\lambda_5| &> -\sqrt{\lambda_1 \lambda_2}. \end{aligned} \tag{30}$$

So the λ parameters are bounded below, and above for the λ_5. The λ parameters are responsible for the masses of the Higgs bosons. Their masses are in the general basis given by

$$m_A^2 = \frac{m_{12}^2}{\sin\beta\cos\beta} - \lambda_5 v^2, \tag{31}$$

$$m_{H^\pm}^2 = m_A^2 + \frac{1}{2} v^2 (\lambda_5 - \lambda_4), \tag{32}$$

$$m_{H,h}^2 = \frac{1}{2}\left(M_{11}^2 + M_{22}^2 \pm \sqrt{\left(M_{11}^2 - M_{22}^2\right)^2 + 4\left(M_{12}^2\right)^2} \right). \tag{33}$$

Where the M^2 is an orthogonal matrix given by

$$M^2 = \begin{pmatrix} m_A^2 s_\beta^2 + v^2(\lambda_1 c_\beta^2 + \lambda_5 s_\beta^2) & s_\beta c_\beta \left[-m_A^2 + v^2(\lambda_3 + \lambda_4)\right] \\ s_\beta c_\beta \left[-m_A^2 + v^2(\lambda_3 + \lambda_4)\right] & m_A^2 c_\beta^2 + v^2(\lambda_2 s_\beta^2 + \lambda_5 c_\beta^2) \end{pmatrix}. \tag{34}$$

So by requiring stability for the potential we get different possible scenarios for the mass spectrum of the Higgs bosons. Note again that the parameter m_{12}^2 is a soft Z_2 breaking term which we will keep non-zero. We specify the values of m_h, m_H, m_A, $m_{H^\pm}$ and m_{12}^2 to get the values of the λ_i's. In the limit $\tan\beta \to \infty$ one gets the relation $m_{12}^2 = s_\beta c_\beta m_H^2$ which we use as an approximation for m_{12}^2. The value of m_{12}^2 does not matter that much, in the end we want the model to satisfy all our conditions and we can adjust m_{12}^2 freely to get the best fit. However this is never necessary with our approximation of m_{12}^2.

For compatibility with [3] we will set $m_{H^\pm}^2 = 500$ GeV and $\tan\beta = 50$. Note however that the precise value of the λ parameters are heavily dependent on the $\tan\beta$ parameter. The λ_i are very sensitive with high values of $\tan\beta$ for which small alterations of other parameters makes them blow up. The choice of $\tan\beta = 50$ will turn out to constrain the masses of the Higgs bosons severely.

Unitarity and Perturbativity

Another constraint on the λ parameters comes from perturbativity. If the couplings in the potential were to become too big, perturbation theory would no longer be possible. Assuming perturbativity thus sets an upper bound on λ_i and to remain in the weakly coupled domain we will use the limit

$$|\lambda_i| < 4\pi. \tag{35}$$

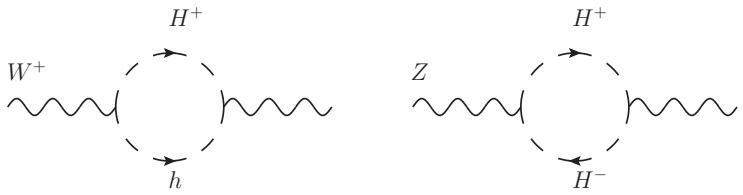

Figure 6: Examples of contributions of the Higgs bosons to the gauge bosons self-energies.

To maintain tree-level unitarity in perturbation theory in vector boson scattering one need to set limits on the eigenvalues of the S-matrix as well. This will further increase the constraints by lowering the upper bounds on the λ_i. A summary of these limits can be found in [9].

Oblique Parameters

Since the 2HDMs introduce new particles that couple to the gauge bosons these can give contributions to electroweak observables. Through loops, the Higgs bosons have to be included in the gauge bosons self-energies, see fig. 6. These contributions can be described by three parameters S,T and U [18]. The experimental bounds on these parameters sets limits on new physics that could affect the electroweak observables. These loop corrections are termed oblique since they do not couple to the external fermions directly but only through the weak interaction indirectly i.e. the propagators.

The details in the calculation of the S, T and U parameters can be found in [19]. Assuming that U=0, both S and T need to be small and the exact limits can be seen in fig. 7.

Since $\tan\beta$ and $m_{H^\pm}$ is fixed for the 2HDM type III of interest we have scanned the parameter space of $m_A - m_H$ to see where the model satisfies the constraints from stability, unitarity and perturbativity. We also made sure that the oblique parameters S and T were within limits. For this we have used the 2HDM calculator [20].

The high value of $\tan\beta = 50$ is needed to fit the 2HDM type III to the B decay data but it also makes the model very unstable with respect to $\sin(\beta-\alpha)$. We assume that the 126 GeV Higgs is the lightest one which means the $\sin(\beta-\alpha)$ parameter has to be close to one. But the allowed regions in the parameter space decrease in size rapidly when choosing any value of $\sin(\beta-\alpha)$ different from 1. The allowed regions of m_H and m_A can be seen in fig. 8 for $\sin(\beta-\alpha)=1$ and in fig. 9 for $\sin(\beta-\alpha)=0.999$.

As can be seen from these plots the $\sin(\beta-\alpha)$ has to be very close to 1. We include the scenario $\sin(\beta-\alpha)=0.85$ in fig. 10 to see how it affects the oblique parameters but with that choice stability, unitarity and perturbativity are not satisfied.

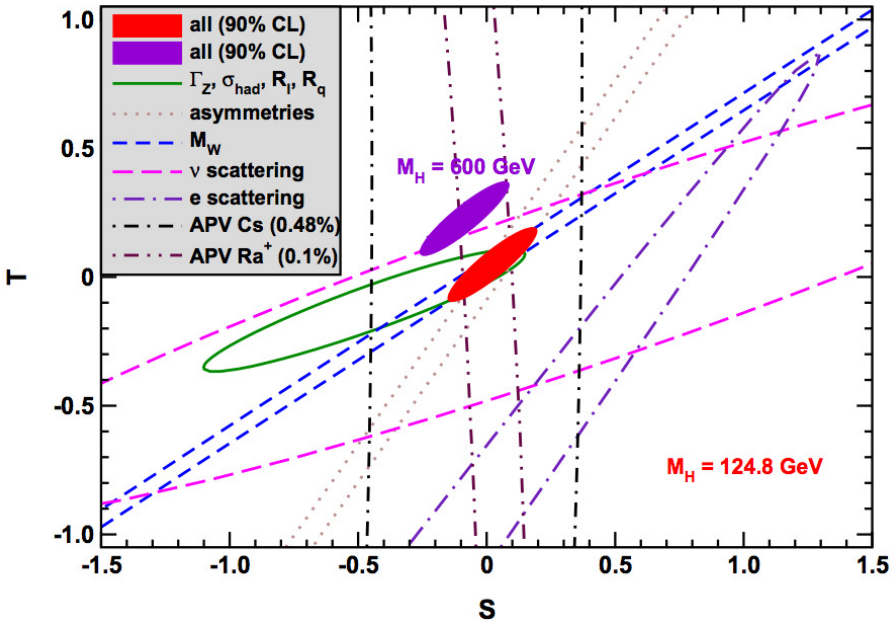

Figure 7: Constraints from experiment on the oblique parameters S and T. The red assumes $m_h = 124.8$ GeV and the violet $m_h = 600$ GeV. Plot taken from [18].

How the stability, unitarity and perturbativity depends on $\tan\beta$ and $\sin(\beta-\alpha)$ can be seen in fig. 11. There the allowed values of $\sin(\beta-\alpha)$ is plotted against the mass of the H and A boson in the case $m_H = m_A$.

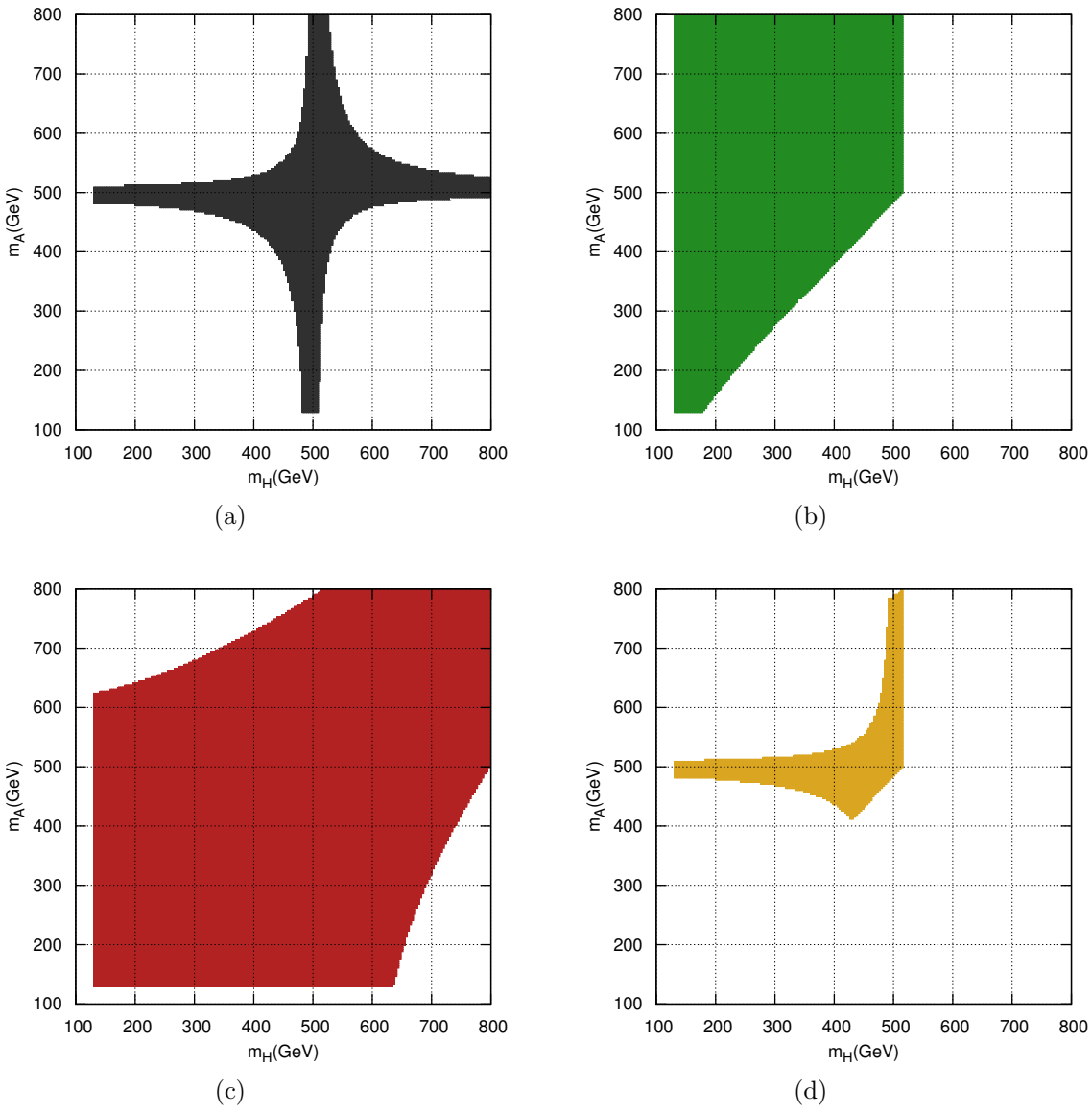

Figure 8: Allowed regions in the parameter space $m_H - m_A$ satisfying the constraints from (a): Oblique parameters S and T (b): Stability (c): Perturbativity (d): All of the above. Unitarity is satisfied for the entire parameter space. Here we assume $m_H, m_A > m_h = 126$ GeV. Note how the requirement that the potential should be bounded restricts a high mass for the m_H. Other parameters that are fixed: $\sin(\beta - \alpha) = 1$, $m_{12}^2 = \sin\beta\cos\beta m_H^2$, $\tan\beta = 50$ and $m_{H^\pm} = 500$ GeV.

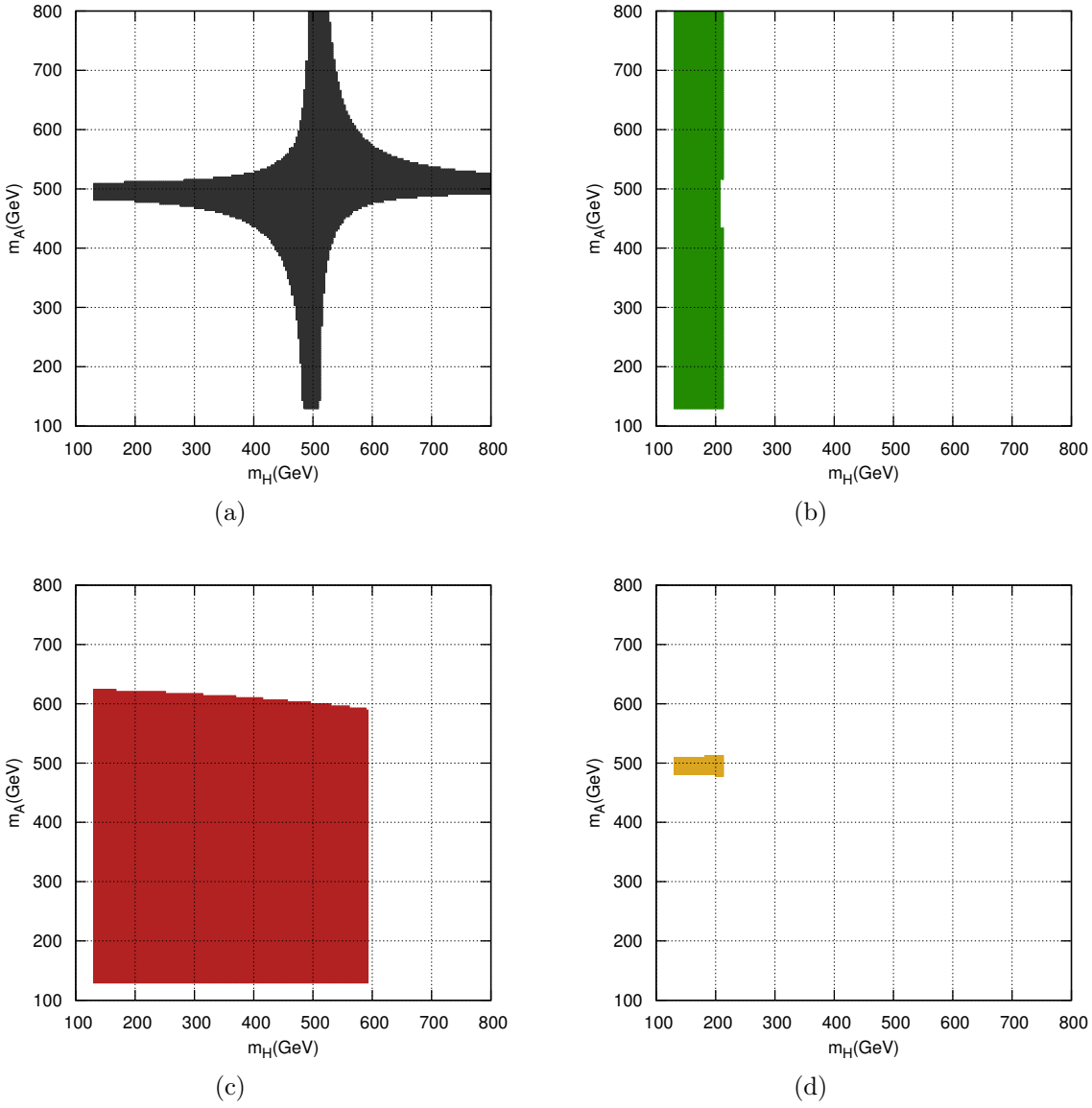

Figure 9: Allowed regions in the parameter space $m_H - m_A$ satisfying the constraints from (a): Oblique parameters S and T (b): Stability (c): Perturbativity (d): All of the above. Unitarity is satisfied for the entire parameter space. There are severe restrictions compared to fig. 8. Here we assume $m_H, m_A > m_h = 126$ GeV. $\sin(\beta - \alpha) = 0.999$, $m_{12}^2 = \sin\beta\cos\beta m_H^2$, $\tan\beta = 50$ and $m_{H^\pm} = 500$ GeV.

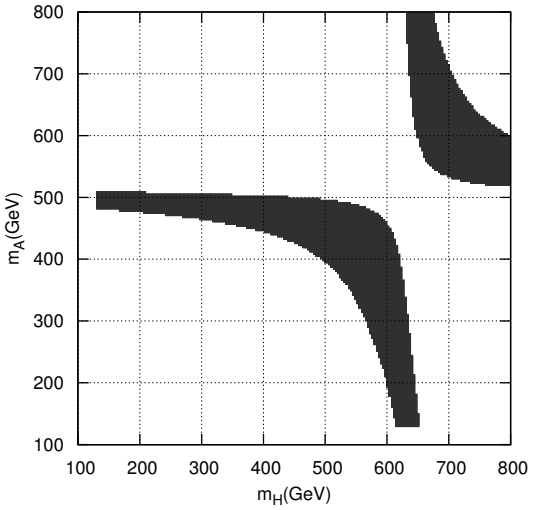

Figure 10: Allowed regions in the $m_H - m_A$ space with respect to the oblique parameters with $\sin(\beta-\alpha) = 0.85$. A heavier H boson is favored. However stability, unitarity and perturbativity are not satisfied. Other parameters that are fixed: $m_{12}^2 = \sin\beta\cos\beta m_H^2$, $\tan\beta = 50$ and $m_{H^\pm} = 500$ GeV.

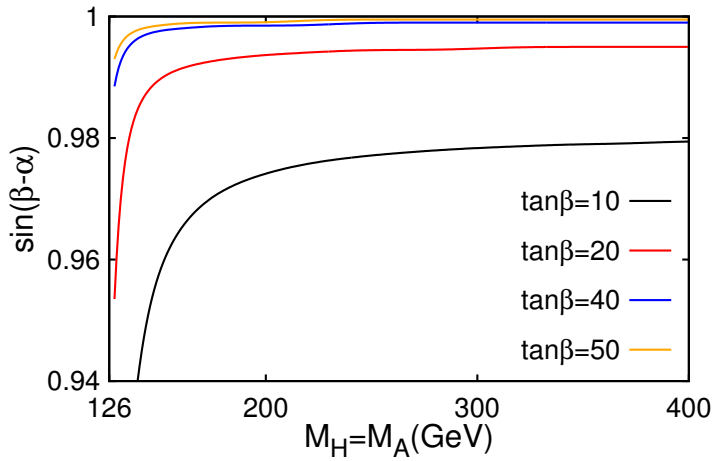

Figure 11: The region above the curves are allowed by stability, unitarity and perturbativity. The x-axis is the mass scale of $m_H = m_A$. Plot done with $m_{12}^2 = \sin\beta\cos\beta m_H^2$, $\tan\beta = 50$ and $m_{H^\pm} = 500$ GeV.

5.2 FCNC in neutral meson mixing

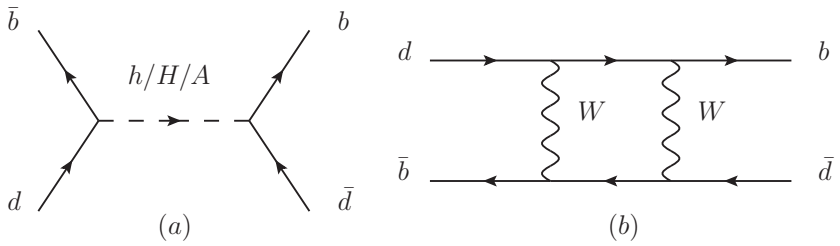

Figure 12: Example of FCNC contributing to $B_d^0 - \bar{B}_d^0$: (a) 2HDM and (b) SM. Note how the FCNC are at tree level in 2HDM but one loop level in SM.

As mentioned several times before the 2HDM type III exhibits FCNC, these have to be within the allowed limits. The most stringent limits are coming from meson mixing that sets boundaries on how large some of the non-diagonal elements of quark mixing can be. Because $F^0 - \bar{F}^0$ mixing is in agreement with the SM this puts severe constraints on the potential tree-level FCNC in 2HDMs, see fig. 12.

The constraints for a general 2HDM from neutral meson mixing can be found in [21],[9]. The mass difference between meson and anti meson can be expressed as:

$$\Delta M_F = \frac{|\rho_{ij}^F|^2}{M_F}\left[S_F\left(\frac{c_{\beta-\alpha}^2}{m_h^2} + \frac{s_{\beta-\alpha}^2}{m_H^2}\right) + \frac{P_F}{m_A^2}\right] \tag{36}$$

$$S_F = \frac{1}{6}B_F f_F^2 M_F^2\left[1 + \frac{M_F^2}{(m_i+m_j)^2}\right] \tag{37}$$

$$P_F = \frac{1}{6}B_F f_F^2 M_F^2\left[1 + \frac{11M_F^2}{(m_i+m_j)^2}\right] \tag{38}$$

Where M_F and m_i is the mass of the meson respectively quarks in question. The f_F is the corresponding decay constant and B_F is the mixing matrix element. These constants are computed using lattice QCD [22], [23] and their numerical values can be found in table 4.

In the following calculation of the limits for ρ^F we require that the 2HDM contributions does not exceed the experimental values by more than 2 standard deviations.

$$\Delta M_F^{SM} + \Delta M_F^{2HDM} \leq \Delta M_F^{expt} + 2\sqrt{\sigma_{SM}^2 + \sigma_{expt}^2} \tag{39}$$

Meson	M_F(GeV)	B_F	f_F(GeV)
$K^0(d\bar{s})$	0.4976 [24]	0.73 ± 0.026 [22]	0.1558 ± 0.0017 [22]
$D^0(\bar{u}c)$	1.8648 [24]	0.82 ± 0.01 [23]	0.165 [23]
$B_d^0(d\bar{b})$	5.2795 [24]	1.26 ± 0.11 [22]	0.1928 ± 0.0099 [22]
$B_s^0(s\bar{b})$	5.3663 [24]	1.33 ± 0.06 [22]	0.2388 ± 0.0095 [22]

Table 4: Parameters for the neutral mesons.

$F^0 - \bar{F}^0$	ΔM_F^{expt}(GeV)	ΔM_F^{SM}(GeV)
$K^0 - \bar{K}^0$	$(3.483 \pm 0.006) \cdot 10^{-15}$ [24]	0
$D^0 - \bar{D}^0$	$1.57^{+0.39}_{-0.415} \cdot 10^{-14}$ [24]	0
$B_d^0 - \bar{B}_d^0$	$(3.344 \pm 0.0197) \cdot 10^{-13}$ [24]	$3.653^{+0.48}_{-0.30} \cdot 10^{-13}$ [25]
$B_s^0 - \bar{B}_s^0$	$(116.668 \pm 0.270) \cdot 10^{-13}$ [26]	$110.6^{+17.1}_{-9.9} \cdot 10^{-13}$ [25]

Table 5: Experimental and theoretical values for the neutral meson mixing.

The masses of the quarks in eq. 36 are the low energy ones defined around 2 GeV. They are listed in table 6. What makes a big difference for the constraints are the masses of the Higgs bosons. Their uncertainty is troublesome and makes the limits vary a lot depending on what the Higgs mass spectrum looks like.

Quark(Energy scale)	Mass(GeV)
m_u(2 GeV)	$2.2 \cdot 10^{-3}$
m_d(2 GeV)	$5 \cdot 10^{-3}$
m_s(2 GeV)	$9.5 \cdot 10^{-2}$
$m_c(m_c)$	1.25
$m_b(m_b)$	4.2

Table 6: Quark masses defined at 2 GeV or at their own mass scale [27].

There are many different scenarios one can imagine for the mass spectrum of the Higgs bosons. We will set $\sin(\beta-\alpha) = 1$ when calculating the constraints. This will get rid of m_h from the calculation and left are the parameters m_H and m_A.

The interesting scenarios for the masses of the heavy neutral Higgs bosons can be seen in fig. 8. We picked three points in the allowed regions in the $m_H - m_A$ space: the two extreme points along the "arms" and one in the middle where $m_H = m_A = 500$ GeV. Increasing the H and A masses also increases the limits on the λ_{ij}^F parameters. Shown below are the limits calculated in these three different scenarios with the Cheng-Sher ansatz. From the K^0, D^0, B_d^0 and B_s^0 mixing we get limits on four of the non-diagonal elements. We put no limits on the other elements which are denoted by $-$.

Scenario 1:

$$m_H = 126 \text{ GeV} \qquad\qquad m_A = 500 \text{ GeV}$$

$$|\lambda^U| \leq \begin{pmatrix} - & 0.35 & - \\ & - & - \\ & & - \end{pmatrix} \qquad |\lambda^D| \leq \begin{pmatrix} - & 0.23 & 0.10 \\ & - & 0.14 \\ & & - \end{pmatrix} \tag{40}$$

Scenario 2:

$$m_H = m_A = 500 \text{ GeV}$$

$$|\lambda^U| \leq \begin{pmatrix} - & 0.57 & - \\ & - & - \\ & & - \end{pmatrix} \qquad |\lambda^D| \leq \begin{pmatrix} - & 0.35 & 0.17 \\ & - & 0.23 \\ & & - \end{pmatrix} \tag{41}$$

Scenario 3:

$$m_H = 500 \text{ GeV} \qquad\qquad m_A = 780 \text{ GeV}$$

$$|\lambda^U| \leq \begin{pmatrix} - & 0.83 & - \\ & - & - \\ & & - \end{pmatrix} \qquad |\lambda^D| \leq \begin{pmatrix} - & 0.52 & 0.24 \\ & - & 0.34 \\ & & - \end{pmatrix} \tag{42}$$

6 RGE evolution

The constraints from the neutral meson mixing does not affect the initial value of ϵ^U_{32} since there is no limit on λ^U_{32}. However if the Yukawa couplings are not protected by symmetry, quantum corrections can generate non-diagonal elements in ρ^F. Thus in the RGE evolution of the Yukawa couplings large non-diagonal elements can affect other non-diagonal elements which may be highly constrained.

In [21] the authors calculated the RGEs for the Yukawa couplings in the 2HDMs and investigated their properties. The equations can be found in Appendix B. Note how the Yukawa couplings are all connected which is the point of worry.

We have used the software in [21] to evolve the Yukawa couplings of the 2HDM type III to see if and when the model breaks the constraints from $F^0 - \bar{F}^0$ mixing. Even though the entire parameter space of ϵ^U_{32} is allowed, it can be very sensitive when it comes to generate non-zero elements in the other Yukawa couplings. The down sector (λ^D) is especially sensitive since it has limits on all its non-diagonal elements. Even though these constraints on the Yukawa couplings are set at the electroweak scale, it is troublesome if the model breaks them at an energy scale a few orders of magnitude above. To explain that one would need to introduce some extra degrees of freedom making the model incomplete. A large sensitivity in the parameter space of ϵ^F can be a sign of fine-tuning making the 2HDM type III an unattractive explanation to the tauonic B meson decays.

More details about the software which was used for the RGE evolution and the input at the electroweak scale can be found in Appendix C.

7 Results

From the constraints on the parameters in the potential, we have investigated the three different mass scenarios, defined in section 5.2. We have used the high value of $\tan\beta = 50$ which makes the model very unstable with respect to $\sin(\beta-\alpha)$ when it comes to bounded potential, unitarity and perturbativity. It practically forces $\sin(\beta-\alpha)$ to be very close to 1. However the value of $\sin(\beta-\alpha)$ does not affect the RGE evolution, only the constraints.

A contour plot of the ϵ_{32}^U parameter space can be seen in fig. 13. It shows at what energy scale the non-diagonal λ^F elements become too large with respect to the limits from $F^0 - \bar{F}^0$ mixing. The plots are symmetrical around origin while the fit of ϵ_{32}^U to the $\mathcal{R}(D^{(*)})$ data in fig. 5 is not. This makes it possible to choose a complex ϵ_{32}^U in the parameter space that is closest to the origin. Then the models FCNC could be within limits all the way up to the grand unification scale($\sim 10^{18}$ GeV) assuming a heavy A boson. The region is however very sensitive and imposing a real ϵ_{32}^U restricts the model by several orders of magnitude.

The FCNC constraints are more severe for lightweight H and A. Scenario 1 with $m_H = 126$ GeV breaks the FCNC limit already at around 1-100 TeV. This clearly favors heavier H and A as expected since that suppresses the tree-level FCNC that were a problem in the first place. One can note that for $\sin(\beta-\alpha) \approx 0.999$, i.e. close but not equal to 1, scenario 1 is the only possible one.

Scenario 2 and 3 are better with a few orders of magnitude and the radius of the contours are expanded as well making it changes less sensitive.

We have used the smallest possible choice of a real value $\epsilon_{32}^U = -0.65$ to see how the individual non-diagonal elements evolve. This choice satisfies the fit to $\mathcal{R}(D)$ and $\mathcal{R}(D^*)$ see fig. 5. One can clearly see that under RGE evolution other non-diagonal elements become sizable. It is mainly the down sector elements that become large. This can be seen if one studies the equations 62 and 63. The non-diagonality spreads in the model to increase the down sector while ϵ_{32}^U decreases. So the large initial value of ϵ_{32}^U does not make itself blow up.

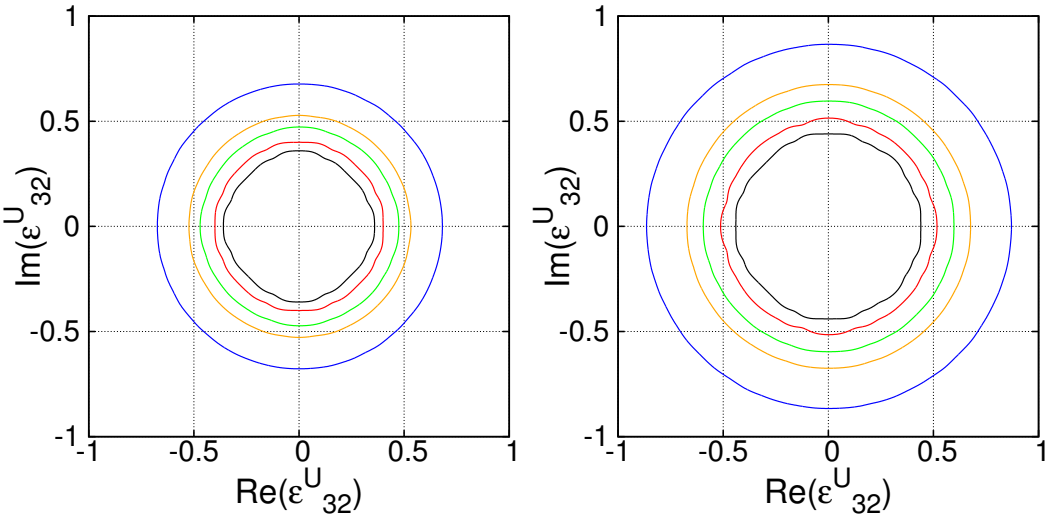

(a)

(b)

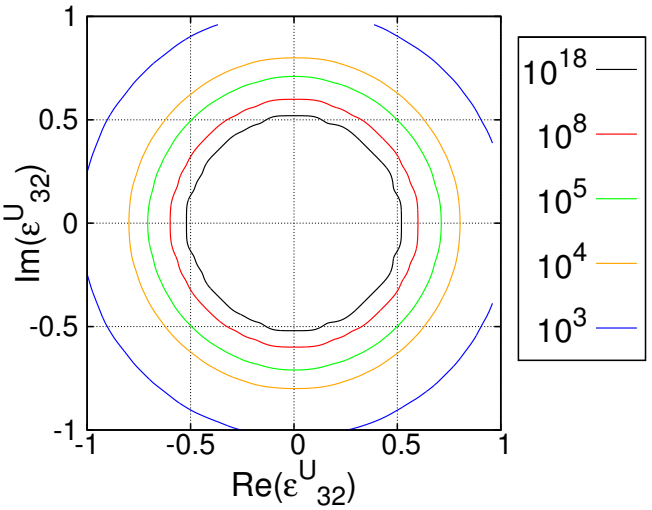

(c)

Figure 13: The energy scale in GeV where non-diagonal elements in $\rho^{U,D}$ becomes bigger than the constraints from $F^0 - \bar{F}^0$ mixing. The three plots are the three different choices of the masses of m_H and m_A. (a): $m_H = 126$ GeV and $m_A = 500$ GeV (b): $m_H = m_A = 500$ GeV (c): $m_H = 500$GeV and $m_A = 780$ GeV. Compare with fig. 5 and note that the allowed region in the parameter space is sensitive to RGE evolution. Parameters used are $\tan\beta = 50$, $\sin(\beta - \alpha) = 1$ and $m_{H^\pm} = 500$ GeV.

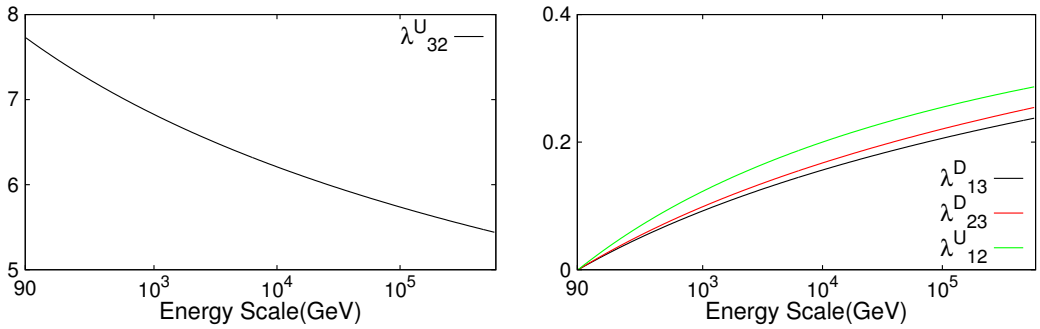

Figure 14: Evolution of individual elements with the Cheng-Sher ansatz. with the initial value $\epsilon^U_{32} = -0.65$. The initial value corresponds to $\lambda^U_{32} \sim 8$ which is very large. Its an order of magnitude bigger than the constraints on the other non-diagonal λ^F elements. The non-diagonal elements that are not included here are small ($< 10^{-3}$). Parameters used are $\tan\beta = 50$, $\sin(\beta - \alpha) = 1$ and $m_{H^\pm} = 500$ GeV.

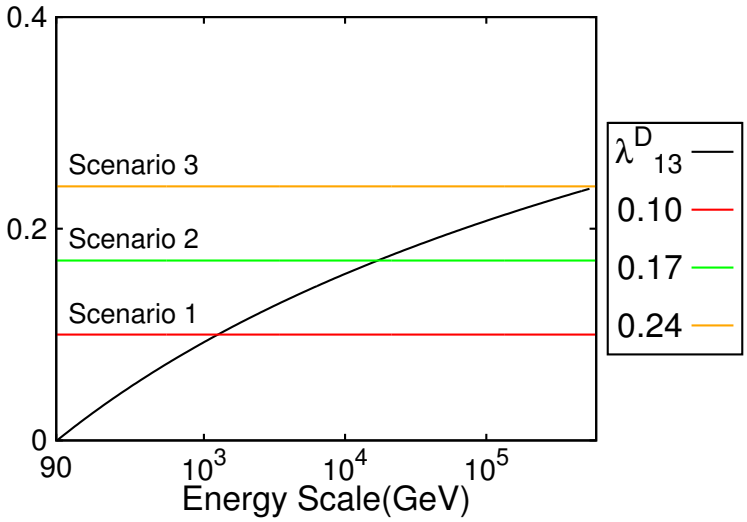

Figure 15: The evolution of λ^D_{13} together with the constraints calculated in section 5.2. This is the element that always reach its limit first. Parameters used are $\tan\beta = 50$, $\sin(\beta - \alpha) = 1$ and $m_{H^\pm} = 500$ GeV.

8 Conclusion

In this thesis we have given a review of how the Higgs mechanism gives masses to the fermions in the SM and the consequences of extending the SM scalar sector to two Higgs doublets instead of one. We discussed the different 2HDMs that could be possible candidates for BSM physics and how to avoid the tree-level FCNC with discrete symmetries.

We have also explained how the data on the decays $B \to D\tau\nu$ and $B \to D^*\tau\nu$ does not agree with the SM and how it can be explained with the 2HDM type III.

To investigate the parameter space of the 2HDM type III we looked at the stability of the vacuum, unitarity and perturbativity of the model. We also looked at the contributions of the 2HDM to the oblique Parameters S and T. It turns out that the value of $\tan\beta = 50$ that is used in [3] makes the model very sensitive with respect to the parameter $\sin(\beta - \alpha)$ which one is almost forced to set to 1. This corresponds to the decoupling limit where the lightest Higgs resembles the SM Higgs. With the choice of $\sin(\beta - \alpha) = 1$ we presented the possible choices of the H and A boson masses.

We calculated the constraints on the FCNC from $F^0 - \bar{F}^0$ mixing in three choices of the H and A boson masses.

And finally we did a RGE evolution of the Yukawa couplings of the model to see whether the model was within limits at higher energies.

To avoid the unwanted FCNC of the 2HDM type III one is forced to suppress the non-diagonal elements of the Yukawa couplings. The constraints from meson mixings are very severe unless the neutral Higgs bosons are very heavy. But the stability, unitarity, perturbativity and limits on the oblique parameters restricts the freedom in choosing m_H and m_A freely. The best case scenario could allow RGE evolution up to $\sim 10^{18}$ GeV if m_H, m_A are above 500 GeV and ϵ^U_{32} takes on the value closest possible to the origin. However that scenario is only possible if $\sin(\beta - \alpha) > 0.9999$. If $\sin(\beta - \alpha)$ is less than that, then both m_H and m_A need to be below 200 GeV. In that case the Yukawa couplings reach their limits already at 1-10 TeV.

Even though the case with only ϵ^U_{32} being non-zero among the non-diagonal elements at the electroweak works out, the RGE evolution show that more concern is justified since the non-diagonality of the Yukawa couplings spreads throughout the flavors. Thus setting sizeable elements in the up sector causes the couplings in the down sector to increase as well. This is probably a big problem if one wants small but non zero elements throughout the sector since then the couplings would increase faster and break the FCNC limits at lower energies. One should note as well that the non-diagonal element that is required to explain the $B \to D^{(*)}\tau\nu$ data with the 2HDM type III is an order of magnitude larger than the limits on the other non-diagonal elements from $F^0 - \bar{F}^0$ mixing.

It is worth mentioning a few words about the stability of the allowed regions in the $m_H - m_A$ space in fig. 8-10 as well. The masses are highly constrained and the allowed region is very narrow. This could likely be a problem if one would do a RGE evolution of the λ_i parameters in the potential. If they are sensitive under

RGE evolution one can easily break stability, unitarity and perturbativity.

In short one could say that the fit of 2HDM type III to the $B \to D^{(*)}\tau\nu$ data requires a high value of $\tan\beta$ and masses of the H and A to be larger than 500 GeV. The choice of parameters seem to be unnatural since there would only be one big non-diagonal element in the Yukawa couplings, without any motivation except explaining the data. This forces $\sin(\beta - \alpha)$ to be close to 1 and the model therefore reaches the decoupling limit where the lightest Higgs boson resembles the SM one.

Appendices

A Effective field theory for 2HDM type III

To calculate the contributions of the charged Higgs to B decays one needs to integrate out the heavy degrees of freedom. This can be done with a operator product expansion. Following the lines of [3] the effective Hamiltonian can be divided into a SM term and the new contributions

$$\mathcal{H}_{\text{eff}} = C_{SM}^{cb} O_{SM}^{cb} + C_R^{cb} O_R^{cb} + C_L^{cb} O_L^{cb} \tag{43}$$

where

$$\begin{aligned} O_{SM}^{cb} &= \bar{c}\gamma_\mu P_L b \bar{\tau}\gamma^\mu P_L \nu_\tau \\ O_R^{cb} &= \bar{c} P_R b \bar{\tau} P_L \nu_\tau \\ O_{SM}^{cb} &= \bar{c} P_L b \bar{\tau} P_L \nu_\tau \end{aligned}$$

and the C functions are the Wilson coefficients:

$$C_{SM}^{cb} = \frac{4G_F V_{cb}}{\sqrt{2}}, \tag{44}$$

$$C_R^{cb} = -\frac{1}{m_{H^\pm}^2} \Gamma_{cb}^{H^\pm LR} \frac{m_\tau}{v} \tan\beta, \tag{45}$$

$$C_L^{cb} = -\frac{1}{m_{H^\pm}^2} \Gamma_{cb}^{H^\pm RL} \frac{m_\tau}{v} \tan\beta, \tag{46}$$

where $\Gamma_{cb}^{H^\pm LR/RL}$ are the couplings in eq. 24.

The contribution from the charged Higgs is contained in the Wilson coefficients C_R and C_L and one can fit them to the data on B decay. This has been done in [3] where they have found the contribution to the SM results to be

$$\mathcal{R}(D) = \mathcal{R}_{SM}(D) \left(1 + 1.5 \cdot \text{Re}\left[\frac{C_R^{cb} + C_L^{cb}}{C_{SM}^{cb}} \right] + 1.0 \left| \frac{C_R^{cb} + C_L^{cb}}{C_{SM}^{cb}} \right|^2 \right), \tag{47}$$

$$\mathcal{R}(D^*) = \mathcal{R}_{SM}(D^*) \left(1 + 0.12 \cdot \text{Re}\left[\frac{C_R^{cb} - C_L^{cb}}{C_{SM}^{cb}} \right] + 0.05 \left| \frac{C_R^{cb} - C_L^{cb}}{C_{SM}^{cb}} \right|^2 \right). \tag{48}$$

The $C_{R,L}^{cb}$ depends on the non-diagonal elements $\epsilon_{U,D}$ so with these equations the 2HDM type III can be fitted to the data on $\mathcal{R}(D)$ and $\mathcal{R}(D^*)$.

B RGEs for 2HDM

The renormalization group equations for the Yukawa couplings in 2HDM can be found in [21]. Using the notation $\mathcal{D} \equiv 16\pi^2 \frac{d}{d(\ln\mu)}$ the RGEs for the Yukawa couplings

in the general basis(the one used in eq. 14) are:

$$\mathcal{D}\eta_k^U = -A_U\eta_k^U + \sum_{l=1}^{2}\Big\{\mathrm{Tr}\left[N_c\left(\eta_k^U\eta_l^{U\dagger} + \eta_l^D\eta_k^{D\dagger}\right) + \eta_k^{L\dagger}\eta_l^L\right]\eta_l^U + \frac{1}{2}\left[\eta_l^U\eta_l^{U\dagger} + \eta_l^D\eta_l^{D\dagger}\right]\eta_k^U + \eta_k^U\eta_l^{U\dagger}\eta_l^U - 2\eta_l^D\eta_k^{D\dagger}\eta_l^U\Big\}, \tag{49}$$

$$\mathcal{D}\eta_k^D = -A_D\eta_k^D + \sum_{l=1}^{2}\Big\{\mathrm{Tr}\left[N_c\left(\eta_k^D\eta_l^{D\dagger} + \eta_l^U\eta_k^{U\dagger}\right) + \eta_k^{L\dagger}\eta_l^L\right]\eta_l^D + \frac{1}{2}\left[\eta_l^U\eta_l^{U\dagger} + \eta_l^D\eta_l^{D\dagger}\right]\eta_k^D + \eta_k^D\eta_l^{D\dagger}\eta_l^D - 2\eta_l^U\eta_k^{U\dagger}\eta_l^D\Big\}, \tag{50}$$

$$\mathcal{D}\eta_k^L = -A_L\eta_k^L + \sum_{l=1}^{2}\Big\{\mathrm{Tr}\left[N_c\left(\eta_k^{U\dagger}\eta_l^U + \eta_k^D\eta_l^{D\dagger}\right) + \eta_k^L\eta_l^{L\dagger}\right]\eta_l^L + \frac{1}{2}\eta_l^L\eta_l^{L\dagger}\eta_k^L + \eta_k^L\eta_l^{L\dagger}\eta_l^L\Big\}, \tag{51}$$

where the A_F are given by the gauge couplings g_1, g_2 and g_3:

$$A_U = 3\frac{(N_c^2-1)}{N_c}g_3^2 + \frac{9}{4}g_2^2 + \frac{17}{12}g_1^2, \tag{52}$$

$$A_D = A_U - g_1^2, \tag{53}$$

$$A_L = \frac{15}{4}g_1^2 + \frac{9}{4}g_2^2. \tag{54}$$

where N_c is the number of colors.

With $\sin\theta_W$ being the weak mixing angle we have $g_1 = e/\cos\theta_W$, $g_2 = e/\sin\theta_W$ and $g_3 = g_s$ and their RGEs are

$$\mathcal{D}(g_1) = \left(\frac{1}{3} + \frac{10}{9}n_q\right)g_1^3 \tag{55}$$

$$\mathcal{D}(g_2) = -\left(7 - \frac{2}{3}n_q\right)g_2^3 \tag{56}$$

$$\mathcal{D}(g_3) = -\frac{1}{3}(11N_c - 2n_q)g_3^3 \tag{57}$$

where n_q is the number of active quarks which is set to 6 in the RGE evolution.

The RGEs for the vacuum expectation values are

$$\mathcal{D}(e^{i\theta_k}v_k) = -\sum_{l=1}^{2}\mathrm{Tr}\left[N_c\left(\eta_k^U\eta_l^{U\dagger} + \eta_l^D\eta_k^{D\dagger}\right) + \eta_l^L\eta_k^{L\dagger}\right]e^{i\theta_l}v_l + \left(\frac{3}{4}g_1^2 + \frac{9}{4}g_2^2\right)e^{i\theta_k}v_k \tag{58}$$

And finally the RGEs of the Yukawa matrices in the Higgs Basis:

$$\begin{aligned}\mathcal{D}(\kappa_0^U) =& -A_U\kappa_0^U + \mathrm{Tr}\left[N_c\left(\kappa_0^U\kappa_0^{U\dagger} + \kappa_0^D\kappa_0^{D\dagger}\right) + \kappa_0^{L\dagger}\kappa_0^L\right]\kappa_0^U \\ &- \frac{1}{2}\tan\beta\mathrm{Tr}\left\{N_c\left(\kappa_0^U\rho_0^{U\dagger} - \rho_0^U\kappa_0^{U\dagger}\right) - N_c\left(\kappa_0^D\rho_0^{D\dagger} - \rho_0^D\kappa_0^{D\dagger}\right) - \left(\kappa_0^L\rho_0^{L\dagger} - \rho_0^L\kappa_0^{L\dagger}\right)\right\}\kappa_0^U \\ &+ \frac{1}{2}\left(\rho_0^U\rho_0^{U\dagger} + \rho_0^D\rho_0^{D\dagger} + \kappa_0^U\kappa_0^{U\dagger} + \kappa_0^D\kappa_0^{D\dagger}\right)\kappa_0^U + \kappa_0^U\left(\rho_0^{U\dagger}\rho_0^U + \kappa_0^{U\dagger}\kappa_0^U\right) \\ &- 2\rho_0^D\kappa_0^{D\dagger}\rho_0^U - 2\kappa_0^D\kappa_0^{D\dagger}\kappa_0^U \end{aligned} \tag{59}$$

$$\begin{aligned}\mathcal{D}(\kappa_0^D) =& -A_D\kappa_0^D + \mathrm{Tr}\left[N_c\left(\kappa_0^U\kappa_0^{U\dagger} + \kappa_0^D\kappa_0^{D\dagger}\right) + \kappa_0^{L\dagger}\kappa_0^L\right]\kappa_0^D \\ &- \frac{1}{2}\tan\beta\mathrm{Tr}\left\{N_c\left(\kappa_0^U\rho_0^{U\dagger} - \rho_0^U\kappa_0^{U\dagger}\right) - N_c\left(\kappa_0^D\rho_0^{D\dagger} - \rho_0^D\kappa_0^{D\dagger}\right) - \left(\kappa_0^L\rho_0^{L\dagger} - \rho_0^L\kappa_0^{L\dagger}\right)\right\}\kappa_0^D \\ &+ \frac{1}{2}\left(\rho_0^U\rho_0^{U\dagger} + \rho_0^D\rho_0^{D\dagger} + \kappa_0^U\kappa_0^{U\dagger} + \kappa_0^D\kappa_0^{D\dagger}\right)\kappa_0^D + \kappa_0^D\left(\rho_0^{D\dagger}\rho_0^D + \kappa_0^{D\dagger}\kappa_0^D\right) \\ &- 2\rho_0^U\kappa_0^{U\dagger}\rho_0^D - 2\kappa_0^U\kappa_0^{U\dagger}\kappa_0^D \end{aligned} \tag{60}$$

$$\begin{aligned}\mathcal{D}(\kappa_0^L) =& -A_L\kappa_0^L + \mathrm{Tr}\left[N_c\left(\kappa_0^{U\dagger}\kappa_0^U + \kappa_0^D\kappa_0^{D\dagger}\right) + \kappa_0^{L\dagger}\kappa_0^L\right]\kappa_0^L \\ &- \frac{1}{2}\tan\beta\mathrm{Tr}\left\{N_c\left(\kappa_0^U\rho_0^{U\dagger} - \rho_0^U\kappa_0^{U\dagger}\right) - N_c\left(\kappa_0^D\rho_0^{D\dagger} - \rho_0^D\kappa_0^{D\dagger}\right) - \left(\kappa_0^L\rho_0^{L\dagger} - \rho_0^L\kappa_0^{L\dagger}\right)\right\}\kappa_0^L \\ &+ \frac{1}{2}\left(\rho_0^L\rho_0^{L\dagger} + \kappa_0^L\kappa_0^{L\dagger}\right)\kappa_0^L + \kappa_0^L\left(\rho_0^{L\dagger}\rho_0^L + \kappa_0^{L\dagger}\kappa_0^L\right) \end{aligned} \tag{61}$$

$$\begin{aligned}\mathcal{D}(\rho_0^U) =& -A_U\rho_0^U + 2\mathrm{Tr}\left[N_c\left(\rho_0^U\kappa_0^{U\dagger} + \kappa_0^D\rho_0^{D\dagger}\right) + \kappa_0^L\rho_0^{L\dagger}\right]\kappa_0^U \\ &+ \mathrm{Tr}\left[N_c\left(\rho_0^U\rho_0^{U\dagger} + \rho_0^D\rho_0^{U\dagger}\right) + \rho_0^L\rho_0^{L\dagger}\right]\rho_0^U \\ &- \frac{1}{2}\cot\beta\mathrm{Tr}\left[N_c\left(\kappa_0^U\rho_0^{U\dagger} + \rho_0^U\kappa_0^{U\dagger}\right) - N_c\left(\kappa_0^D\rho_0^{D\dagger} - \rho_0^D\kappa_0^{D\dagger}\right) - \left(\kappa_0^L\rho_0^{L\dagger} - \rho_0^L\kappa_0^{L\dagger}\right)\right]\rho_0^U \\ &+ \frac{1}{2}\left(\rho_0^U\rho_0^{U\dagger} + \rho_0^D\rho_0^{D\dagger} + \kappa_0^U\kappa_0^{U\dagger} + \kappa_0^D\kappa_0^{D\dagger}\right)\rho_0^U + \rho_0^U\left(\rho_0^{U\dagger}\rho_0^U + \kappa_0^{U\dagger}\kappa_0^U\right) \\ &- 2\rho_0^D\rho_0^{D\dagger}\rho_0^U - 2\kappa_0^D\rho_0^{D\dagger}\kappa_0^U \end{aligned} \tag{62}$$

$$\begin{aligned}\mathcal{D}(\rho_0^D) =& -A_D\rho_0^D + 2\mathrm{Tr}\left[N_c\left(\kappa_0^U\rho_0^{U\dagger} + \rho_0^D\kappa_0^{D\dagger}\right) + \rho_0^L\kappa_0^{L\dagger}\right]\kappa_0^D \\ &+ \mathrm{Tr}\left[N_c\left(\rho_0^U\rho_0^{U\dagger} + \rho_0^D\rho_0^{U\dagger}\right) + \rho_0^L\rho_0^{L\dagger}\right]\rho_0^D \\ &+ \frac{1}{2}\cot\beta\mathrm{Tr}\left[N_c\left(\kappa_0^U\rho_0^{U\dagger} + \rho_0^U\kappa_0^{U\dagger}\right) - N_c\left(\kappa_0^D\rho_0^{D\dagger} - \rho_0^D\kappa_0^{D\dagger}\right) - \left(\kappa_0^L\rho_0^{L\dagger} - \rho_0^L\kappa_0^{L\dagger}\right)\right]\rho_0^D \\ &+ \frac{1}{2}\left(\rho_0^U\rho_0^{U\dagger} + \rho_0^D\rho_0^{D\dagger} + \kappa_0^U\kappa_0^{U\dagger} + \kappa_0^D\kappa_0^{D\dagger}\right)\rho_0^D + \rho_0^D\left(\rho_0^{U\dagger}\rho_0^U + \kappa_0^{U\dagger}\kappa_0^U\right) \\ &- 2\rho_0^U\rho_0^{U\dagger}\rho_0^D - 2\kappa_0^U\rho_0^{U\dagger}\kappa_0^D \end{aligned} \tag{63}$$

$$
\begin{aligned}
\mathcal{D}(\rho_0^L) = &- A_L\rho_0^L + 2\mathrm{Tr}\left[N_c\left(\kappa_0^U\rho_0^{U\dagger} + \rho_0^D\kappa_0^{D\dagger}\right) + \rho_0^L\kappa_0^{L\dagger}\right]\kappa_0^L \\
&+ \mathrm{Tr}\left[N_c\left(\rho_0^U\rho_0^{U\dagger} + \rho_0^D\rho_0^{U\dagger}\right) + \rho_0^L\rho_0^{L\dagger}\right]\rho_0^L \\
&+ \frac{1}{2}\cot\beta\mathrm{Tr}\left[N_c\left(\kappa_0^U\rho_0^{U\dagger} + \rho_0^U\kappa_0^{U\dagger}\right) - N_c\left(\kappa_0^D\rho_0^{D\dagger} - \rho_0^D\kappa_0^{D\dagger}\right) - \left(\kappa_0^L\rho_0^{L\dagger} - \rho_0^L\kappa_0^{L\dagger}\right)\right]\rho_0^L \\
&+ \frac{1}{2}\left(\rho_0^L\rho_0^{L\dagger} + \kappa_0^L\kappa_0^{L\dagger}\right)\rho_0^L + \rho_0^L\left(\rho_0^{L\dagger}\rho_0^L + \kappa_0^{L\dagger}\kappa_0^L\right) \qquad (64)
\end{aligned}
$$

C Input for RGE evolution

The RGE evolution was performed with a software used in [21]. By discretization it solves the RGE equations and evolve all the parameters to higher energies. In each step of the evolution, it diagonalize the κ^F matrices to keep the masses on the diagonal. The program uses C++ libraries *Eigen* and *GSL* to solve matrix operations and ordinary differential equations with the Runge-Kutta-Fehlberg method.

The evolution starts at the electroweak scale $\mu = 91.186$ GeV and thus needs the appropriate input. The fermion masses are taken from [27] and are in GeV:

$$
\begin{array}{lll}
m_u = 1.29\cdot 10^{-3} & m_c = 0.619 & m_t = 171.7 \\
m_d = 2.93\cdot 10^{-3} & m_s = 0.055 & m_b = 2.89 \\
m_e = 0.487\cdot 10^{-3} & m_\mu = 0.103 & m_\tau = 1.746
\end{array}
$$

In diagonalizing the Yukawa couplings (κ^F matrices) the PDG phase convention was used for the V_{CKM} matrix.

$$
V_{CKM} = \begin{pmatrix}
c_{12}c_{13} & s_{12}c_{13} & s_{13}e^{-i\delta} \\
-s_{12}c_{23} - c_{12}s_{23}s_{13}e^{i\delta} & c_{12}c_{23} - s_{12}s_{23}s_{13}e^{i\delta} & s_{23}c_{13} \\
s_{12}s_{23} - c_{12}c_{23}s_{13}e^{i\delta} & -c_{12}s_{23} - s_{12}c_{23}s_{13}e^{i\delta} & c_{23}c_{13}
\end{pmatrix}
$$

Where

$$
s_{12} = \lambda \qquad s_{23} = A\lambda^2 \qquad s_{13}e^{i\delta} = \frac{A\lambda^3(\bar\rho + i\bar\eta)\sqrt{1 - A^2\lambda^4}}{\sqrt{1-\lambda^2}\left[1 - A^2\lambda^4(\bar\rho + i\bar\eta)\right]}
$$

$$
\lambda = 0.2253 \qquad A = 0.808 \qquad \bar\rho = 0.132 \qquad \bar\eta = 0.341
$$

And other parameters used are

$$
\begin{aligned}
v^2 &= \frac{1}{\sqrt{2}G_F} \\
G_F &= 1.16637\cdot 10^{-5}\ \mathrm{GeV}^{-2} \\
\alpha \equiv \frac{e^2}{4\pi} &= \frac{1}{127.91} \\
\alpha_s \equiv \frac{g_3^2}{4\pi} &= 0.118 \\
\sin^2\theta_W &= 0.2233
\end{aligned}
$$

References

[1] **ATLAS Collaboration** Collaboration, G. Aad et al., *Observation of a new particle in the search for the Standard Model Higgs boson with the ATLAS detector at the LHC*, *Phys.Lett.* **B716** (2012) 1–29, [arXiv:1207.7214].

[2] **CMS Collaboration** Collaboration, S. Chatrchyan et al., *Observation of a new boson at a mass of 125 GeV with the CMS experiment at the LHC*, *Phys.Lett.* **B716** (2012) 30–61, [arXiv:1207.7235].

[3] A. Crivellin, C. Greub, and A. Kokulu, *Explaining $B \to D\tau\nu$, $B \to D^*\tau\nu$ and $B \to \tau\nu$ in a 2HDM of type III*, *Phys.Rev.* **D86** (2012) 054014, [arXiv:1206.2634].

[4] **BaBar Collaboration** Collaboration, J. Lees et al., *Evidence for an excess of $\bar{B} \to D^{(*)}\tau^-\bar{\nu}_\tau$ decays*, *Phys.Rev.Lett.* **109** (2012) 101802, [arXiv:1205.5442].

[5] M. E. Peskin and D. V. Schroeder, *An Introduction to quantum field theory*, .

[6] A. Zee, *Quantum field theory in a nutshell*, .

[7] G. L. Kane, *MODERN ELEMENTARY PARTICLE PHYSICS*, .

[8] *http://laplacian.wordpress.com/2010/05/16/the-higgs-particle-for-semi-dummies/*, .

[9] G. Branco, P. Ferreira, L. Lavoura, M. Rebelo, M. Sher, et al., *Theory and phenomenology of two-Higgs-doublet models*, *Phys.Rept.* **516** (2012) 1–102, [arXiv:1106.0034].

[10] J. F. Gunion, H. E. Haber, G. L. Kane, and S. Dawson, *The Higgs Hunter's Guide*, *Front.Phys.* **80** (2000) 1–448.

[11] S. L. Glashow and S. Weinberg, *Natural Conservation Laws for Neutral Currents*, *Phys.Rev.* **D15** (1977) 1958.

[12] T. Cheng and M. Sher, *Mass Matrix Ansatz and Flavor Nonconservation in Models with Multiple Higgs Doublets*, *Phys.Rev.* **D35** (1987) 3484.

[13] J. F. Kamenik and F. Mescia, *$B \to t$; D tau nu Branching Ratios: Opportunity for Lattice QCD and Hadron Colliders*, *Phys.Rev.* **D78** (2008) 014003, [arXiv:0802.3790].

[14] S. Fajfer, J. F. Kamenik, and I. Nisandzic, *On the $B \to D^*\tau\bar{\nu}_\tau$ Sensitivity to New Physics*, *Phys.Rev.* **D85** (2012) 094025, [arXiv:1203.2654].

[15] A. Crivellin, A. Kokulu, and C. Greub, *Flavor-phenomenology of two-Higgs-doublet models with generic Yukawa structure*, *Phys.Rev.* **D87** (2013) 094031, [arXiv:1303.5877].

[16] G. Degrassi, S. Di Vita, J. Elias-Miro, J. R. Espinosa, G. F. Giudice, et al., *Higgs mass and vacuum stability in the Standard Model at NNLO*, *JHEP* **1208** (2012) 098, [arXiv:1205.6497].

[17] I. Ivanov, *Minkowski space structure of the Higgs potential in 2HDM*, *Phys.Rev.* **D75** (2007) 035001, [hep-ph/0609018].

[18] J. Erler, *Electroweak tests of the Standard Model*, arXiv:1208.6262.

[19] H. E. Haber and D. O'Neil, *Basis-independent methods for the two-Higgs-doublet model III: The CP-conserving limit, custodial symmetry, and the oblique parameters S, T, U*, *Phys.Rev.* **D83** (2011) 055017, [arXiv:1011.6188].

[20] D. Eriksson, J. Rathsman, and O. Stal, *2HDMC: Two-Higgs-Doublet Model Calculator Physics and Manual*, *Comput.Phys.Commun.* **181** (2010) 189–205, [arXiv:0902.0851].

[21] J. Bijnens, J. Lu, and J. Rathsman, *Constraining General Two Higgs Doublet Models by the Evolution of Yukawa Couplings*, *JHEP* **1205** (2012) 118, [arXiv:1111.5760].

[22] J. Laiho, E. Lunghi, and R. S. Van de Water, *Lattice QCD inputs to the CKM unitarity triangle analysis*, *Phys.Rev.* **D81** (2010) 034503, [arXiv:0910.2928].

[23] E. Lunghi and A. Soni, *Footprints of the Beyond in flavor physics: Possible role of the Top Two Higgs Doublet Model*, *JHEP* **0709** (2007) 053, [arXiv:0707.0212].

[24] **Particle Data Group** Collaboration, K. Nakamura et al., *Review of particle physics*, *J.Phys.* **G37** (2010) 075021.

[25] A. Lenz, U. Nierste, J. Charles, S. Descotes-Genon, A. Jantsch, et al., *Anatomy of New Physics in $B - \bar{B}$ mixing*, *Phys.Rev.* **D83** (2011) 036004, [arXiv:1008.1593].

[26] **LHCb Collaboration** Collaboration, L. Collaboration, *Measurement of Δm_s in the decay $B_s^0 \to D_s^-(K^+K^-\pi^-)\pi^+$ using opposite-side and same-side flavour tagging algorithms*, .

[27] Z.-z. Xing, H. Zhang, and S. Zhou, *Updated Values of Running Quark and Lepton Masses*, *Phys.Rev.* **D77** (2008) 113016, [arXiv:0712.1419].